Biogeochemical responses to mixing of glacial meltwater and hot spring discharge in the Mount St. Helens crater

A. Dubnick[1], Q. Faber [2], J. R. Hawkings[3], N. Bramall[4], B. C. Christner [2], P. T. Doran[5], J. Nadeau[6], C. Snyder [6], A. M. Kellerman[7], A. M. McKenna[8,9], R. G. M. Spencer[7], M. L. Skidmore[1]

[1]Department of Earth Sciences, Montana State University, Bozeman, Montana, USA

[2]Department of Microbiology and Cell Science, University of Florida, Gainesville, Florida, USA

[3]Department of Earth and Environmental Science, University of Pennsylvania, Philadelphia, Pennsylvania, USA.

[4]Leiden Measurement Technology LLC, Sunnyvale, California, USA

[5] Department of Geology and Geophysics, Louisiana State University, Baton Rouge, Louisiana, USA

[6] Department of Physics, Portland State University, Portland, Oregon, USA

[7]National High Magnetic Field Laboratory Geochemistry Group and Department of Earth, Ocean and Atmospheric Science, Florida State University, Tallahassee, Florida, USA.

[8]National High Magnetic Field Laboratory, Florida State University, Tallahassee, Florida, USA.

[9] Department of Soil and Crop Sciences, Colorado State University, Fort Collins, Colorado 80523-1170, United States

Corresponding author: Ashley Dubnick (ashley.dubnick@montana.edu)

Key Points:

- Glacier and hot spring discharge contained distinct major ion, trace element, dissolved organic matter (DOM) and biological signatures.
- Many of the chemical species from the glacier remained in solution after the waters mixed, but many of those from the hot spring did not.
- Mixed waters supported seston and benthic ecosystems that had higher phototrophic and microbial biomass than either of the water sources.

This article has been accepted for publication and undergone full peer review but has not been through the copyediting, typesetting, pagination and proofreading process, which may lead to differences between this version and the Version of Record. Please cite this article as doi: 10.1029/2022JG006852.

Abstract

Environments where geothermal waters and glacier meltwater mix are common on Earth, yet little is known about the biogeochemical processes that occur when hot, reduced geothermal water mixes with cold, oxidized glacial meltwater in natural systems. Mount St. Helens provides an ideal location to study the interaction between geothermal and glacier waters since the water sources, and their mixing environment in Step Creek, are exposed in the volcanic crater. We find that the two water sources contain distinct major ion, trace element, dissolved organic matter (DOM) and biological signatures. The hot spring contains high concentrations of biogeochemically-reactive components (e.g. siderophile and chalcophile trace elements and DOM) compared to the glacier discharge, but a large fraction of these solutes do not remain in solution after the waters mix. In contrast, glacier discharge contains fewer solutes, but most of these solutes remain in solution after the waters mix. The mixing of glacier and hot spring water in Step Creek supports seston and benthic ecosystems that have higher phototrophic and microbial biomass than those in the source waters, suggesting that the mixing environment in this high-gradient stream provide a more comprehensive suite of soluble and essential nutrients that promote primary production and DOM cycling.

Plain Language Summary

Most of the waters that drain from the crater of Mount St. Helens originate from hot spring seeps or the glacier within the crater. We found these two water sources have distinct chemical fingerprints. When the two water types mix in Step Creek, many of the chemical species from the hot spring either precipitate out of solution or are consumed by the aquatic ecosystem, while most of the chemical species from the glacier flow downstream. The chemical energy and the combination of essential nutrients supplied by the two water sources appears to stimulate a more productive downstream aquatic ecosystem.

1. Introduction

The mixing of geothermal waters and glacier meltwater is a widespread phenomenon, but its chemical and microbiological effects on water quality are not fully understood. Approximately one fifth of the 1,443 known subaerial Holocene volcanic centers are glaciated or have permanent snowfields (Curtis & Kyle, 2017). These glaciated volcanoes occur on every continent and are particularly prominent in plate-boundary and hotspot volcanic regions including, for example, the Cascades of the American northwest, Alaska, the Andes, Iceland, and the Kamchatka peninsula of Russia (Curtis & Kyle, 2017). Furthermore, subglacial volcanoes and geothermal heat are renowned for producing large quantities of meltwater that can result in glacial outburst floods, as is commonly observed in Iceland (Björnsson, 2002; Tomasson, 1996) and other regions around the world (Major & Newhall, 1989; Pierson et al., 1990). Volcanoes and geothermal sites are widespread in the heavily glaciated region of Antarctica, including at high elevations and along the margins of the continent in ice-free terrain (Fraser et al., 2014), as well as beneath the West Antarctic Ice Sheet, where 138 volcanoes have been identified (De Vries et al., 2018). Similar systems may also exist on other planetary bodies. For example, volcanism and glaciation have been dominant processes on Mars and high-resolution imagery

and topographic data reveal landforms indicative of volcano-ice interactions (Neukum et al., 2004; Orosei et al., 2018; Scanlon et al., 2014).

Warm geothermal waters usually contain high concentrations of reduced volcanic gases and solute, while cold glacial meltwaters are typically solute-poor and oxic. Mixing between these two water and solute sources can have important biogeochemical implications. First, the mixing rates between the two water sources can define downstream physicochemical conditions, including redox state, solute composition and the concentration of volatile gases (Burns et al., 2018; P. M. Wynn et al., 2015) and thus the microbial processes that can occur. For example, geothermal activity beneath the Icelandic glacier Sólheimajökull creates sub-oxic conditions that promotes methane production along the downstream subglacial flow path (Burns et al., 2018). Second, the mixing of such chemically-distinct water types may provide chemical disequilibrium that microorganisms can use to fuel their metabolism. For example, the microbes detected in a subglacial volcanic crater lake system in Iceland were related to microbes capable of using sulfide, sulfur or hydrogen (common geothermal components) as electron donors and oxygen, sulfate or carbon dioxide (common glacier components) as electron acceptors (Gaidos et al., 2009). Since the mixing of geothermal waters and glacier meltwater can provide life's basic requirements, such environments are high priority targets in the search for extraterrestrial life (Garcia-Lopez & Cid, 2017; Schulze-Makuch et al., 2007) and have been studied in analog research on Earth (Gaidos et al., 2004, 2009; Moreras- Marti et al., 2021).

Previous field studies suggest that volcanic chemical species are important energy and nutrient sources for cryospheric ecosystems, including snow algae communities of stratovolcanoes of the Pacific Northwest (Hamilton & Havig, 2016; Havig & Hamilton, 2019), the englacial microbial communities of a glaciated volcano on Deception Island, Antarctica (Martinez-Alonso et al., 2019), and subglacial volcanic crater lake (Gaidos et al., 2004, 2009) and glacially-fed ponds (Moreras- Marti et al., 2021) in Iceland. However, the nature of these systems often precludes access to the discrete mixing environments that exist and/or their volcanic and cryospheric endmembers. For this reason, Mount St. Helens provides an ideal location to study the interaction between glacial meltwater and geothermal waters since glacial and geothermal water sources and their mixing environment are exposed as surface waters in the crater.

Mount St. Helens has been studied extensively since its eruption in 1980, including research on its volcanology and petrology (Pallister et al., 2008; Wanke et al., 2019), geology (Gabrielli et al., 2020), the Crater Glacier in which recent dacite domes protrude (Price & Walder, 2007; Walder et al., 2007, 2010), groundwater systems (Bedrosian et al., 2007; J. Wynn et al., 2016), and hydrothermal crater discharge (Bergfeld et al., 2008, 2017; Goff & McMurtry, 2000; Shevenell & Goff, 1993; Thompson, 1990). These studies provide a framework for understanding the volcanic and glacial histories of the two primary water sources that mix and are discharged from the crater. The objective of this study is therefore to (1) characterize the nutrients, chemical energy sources, and biomass associated with geothermal and glacial waters using integrated interdisciplinary analytical techniques, and (2) evaluate the biogeochemical and microbiological effects as these waters mix.

2 Materials and Methods

2.1 Field Site

The catastrophic eruption of Mount St. Helens volcano in 1980 removed the upper 400 m of the mountain, leaving a crater 2 km x 3.5 km in size (Christiansen & Peterson, 1981). During the eruption, a debris avalanche breached the crater to flow down the north flank, flattening the surrounding landscape and covering the area with fresh ash, pumice and volcanic rocks (Christiansen & Peterson, 1981). In response to heavy snowfalls and frequent rock and snow debris avalanches from the crater walls, a glacier formed in the shadow along the southern rim of the crater. Dacite domes from the 1980-1984 eruption, and another that followed in 2004-2008, protrude Crater Glacier, splitting the glacier into two arms. The highly crevassed glacier quickly channels meltwater to the glacier bed, where it likely drains in the shallow subsurface amongst the thick layer of coarse rock debris underlying the glacier, largely comprised of 1980 avalanche and pyroclastic deposits (Walder et al., 2010) consisting of dacite, andesite and basalt (Glicken, 1996).

Step Creek drains the western arm of the glacier (Figure 1), with discharge rates that typically peak in July/August >700 L/s) and recede to a baseline flow rate (~200 L/s) throughout the winter (Bergfeld et al., 2008). Approximately 500 m downstream from the glacier terminus, a set of hot springs emerge from the subsurface either directly into the stream bed, or in one case, the stream bank within 3 meters of the creek.. The springs are thought to drain through a perched aquifer at 60-120 m depth, within or at the base of the 1980 debris avalanche deposits (Shevenell & Goff, 1993). These thermal waters probably originate in a hydrothermal system within the lava dome where water vapor is exsolved from deep cooling magma, condenses at shallower depths where it mixes with meteoric waters and interacts with the still-hot dacite intrusive rock (Bedrosian et al., 2007; Wynn et al., 2016).

2.2 Field Methods

We visited the Step Creek watershed on September 21 and 28, 2020, a time of year in which discharge rates from the crater have receded from their peak in July/August (Bergfeld et al., 2008) and glacial runoff is dominated by ice-melt rather than snow-melt. Over the two days, we collected one sample of each of the following (i) the glacier discharge in Step Creek, approximately 100 m from the terminus (hereafter referred to as ‘glacier’ discharge), (ii) the hot spring discharge draining into Step Creek (hereafter referred to as ‘hot spring’ discharge), and (iii) the mixed waters as well as benthic mats in Step Creek (hereafter referred to as ‘Mixed Downstream’) (Figure 1), approximately 2 km downstream, after the waters flow over a waterfall. We also sampled benthic biofilms and mats from Step Creek, where the hot spring and glacier waters first mix (hereafter referred to as ‘Mixed Upstream’) (Figure 1). In-situ temperature and electrical conductivity measurements were collected along the upper reach of Step Creek, including five hot spring discharge locations, as well as the Mixed Downstream sampling site using an Onset® HOBO® U-24-001 conductivity logger. In-situ pH measurements were collected using a handheld pH meter (Oakton®).

Field and storage methods for aqueous chemistry and seston biomass sampling are described in Table S1. In brief, a peristaltic pump or syringe were used to filter water samples for (1) DOM characterization via negative-ion electrospray ionization Fourier transform ion cyclotron resonance mass spectrometry (FT-ICR MS) (Hendrickson et al., 2015; Smith et al.,

2018), (2) Dissolved organic carbon (DOC), (3) major ions and nutrients, (4) alkalinity, and (5) size fractionated trace metals. The two trace metal size fractions are referred to as colloidal/nanoparticle (cn[element], 0.02 - 0.22 µm) and soluble (s[element], <0.02 µm), as per previous naming conventions (Hawkings et al., 2020), with dissolved (d[element]) considered as the fraction <0.22 µm. Unfiltered samples were also collected to measure fluorescent DOM and cell densities, and samples were filtered in the field with syringe and Nalgene^{TM} Filter tower for seston microbial biomass and primary producer biomass, respectively (Table S1).

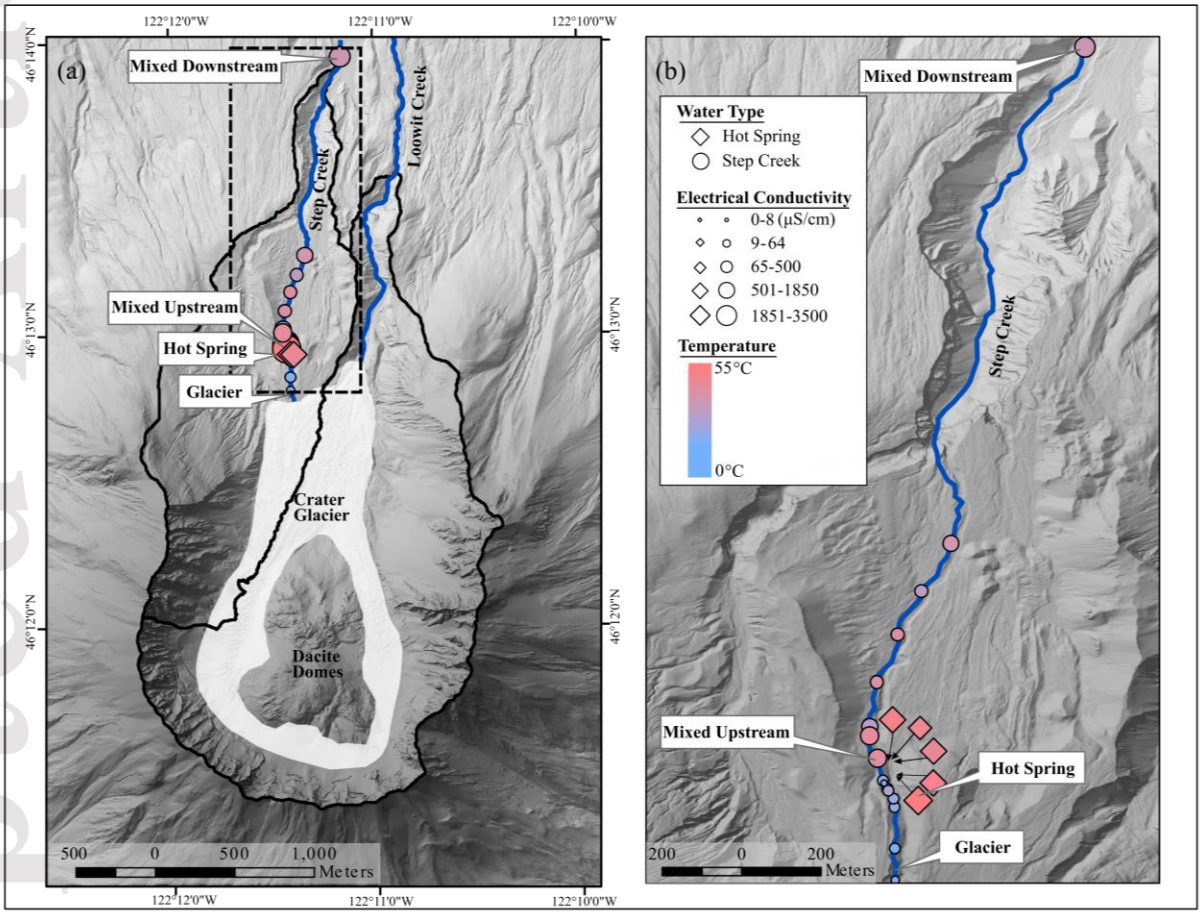

Figure 1: (a) Map of Mount St. Helens study area including the two watersheds (solid black lines) and creeks (solid blue lines) that drain the crater and sample locations along Step Creek ('glacier', 'hot spring', 'Mixed Upstream' and 'Mixed Downstream'), and discrete conductivity and temperature measurements along Step Creek. (b) Detailed view (covering area indicated by the dashed box in panel (a)) showing sample and survey locations along Step Creek. The legend applies to both panels. Basemap derived from Mosbrucker (2014).

Biofilms for pigment analysis were collected using sterile scoops, placed into 50 mL conical tubes, chilled in the field, and stored at -20°C until processed. Biofilms for microscopy were stored at 1-4 ºC until imaged. Digital holographic microscopy (DHM) was performed in the field (for glacier discharge samples) or with returned samples (within 72 hrs) in the laboratory (for biofilm) using a custom instrument based upon a previously described off-axis, common-

path design (Wallace et al., 2016). The instrument size was reduced relative to the original design by "folding" the optical train and modified for field use by interfacing it to an electronics card that allowed for push-button operation and battery power. The sample chambers were 0.8 mm deep and the lateral view was 365x365 µm and the spatial resolution was ~0.8 µm. Data were collected using a custom software package (DHMx) available from an open source (Fregoso, 2020). Data analysis was performed using a Fiji reconstruction package (Cohoe et al., 2019). Tracking was performed by median subtraction of the holograms followed by reconstruction in amplitude (Bedrossian et al., 2020). There was no appreciable fluid flow in the sample chamber during image capture.

2.3 Laboratory Methods

Samples were analyzed for major ions (F^-, Cl^-, NO_2^-, Br^-, NO_3^-, PO_4^{3-}, SO_4^{2-}, NH_4^+, Na^+, Mg^{2+} and Ca^{2+}) by ion chromatography using a Metrohm Compact IC Flex ion chromatograph equipped with a C4 cation column and an aSupp5 anion column; precision and accuracy were better than 5%. Alkalinity was measured by manually titrating approximately 40 ml of sample with 0.0016N or 0.00016 H_2SO_4 and recording the pH at regular intervals. Trace metal samples were measured on a Thermo Scientific™ Element 2™ HR-ICP-MS (high resolution inductively coupled mass spectrometer) using In as an internal standard to correct for drift and matrix effects, following methods described by Hawkings et al., (2020). Precision and accuracy were determined using gravimetrically-weighed standards and replicates of a certified reference material (SLRS-6; National Research Council of Canada), and were better than ±5 %, apart from La, Ce, Pr, Nd and Pb, with accuracy varying between ±8 – 12 %. DOC concentrations were measured as non-purgeable organic carbon, after sample acidification with 12 M HCl to pH 2, using a Shimadzu™ TOC-L high temperature catalytic combustion analyzer with high sensitivity catalyst. Sample concentrations were determined from an average of three injections (out of five) against a 6-point calibration curve ranging from 0 – 2000 ppb DOC, with a coefficient of variance <5 %. Solid-phase extracted DOM (SPE-DOM) composition was determined after extraction onto and subsequent elution from PPL (Priority PolLutant) resin (Agilent Technologies) and analyzed by negative-ion electrospray ionization with a custom-built 21 tesla FT ICR-MS (Hendrickson et al., 2015; Smith et al., 2018), following sample preparation and analytical procedures described by Kellerman et al. (2021).

Samples for FDOM were analyzed using the bespoke Sub-glacial Underwater Reconnaissance Flow-through Fluorescence Spectrometer (SURFFS), a six-channel flow-through analyzer originally developed for a glacier penetrating cryobot, VALKYRIE (Very deep Autonomous Laser-powered Kilowatt-class Yo-yoing Robotic Ice Explorer) (Clark et al., 2018). Fluorescence of the water samples was excited by 255-nm LEDs with emission monitored simultaneously to detect protein-like material (320 nm and 340 nm), fulvic acid/clay material (375 nm and 500 nm) and volcanic ash/chlorophyll material (675 nm) (Bramall, 2007; Dartnell et al., 2010; Eshelman et al., 2019; Price et al., 2009). Sample water was pressure driven using nitrogen gas from the sample bottles to the fluorometer and the flow rate of the fluid was monitored on the output. Each data point presented herein represents the average of several hundred readings of the fluid flowing through the SURFFS instrument. Between samples, the system was cleaned using a solution of DIW and Five Star PBW™ cleaner and finally rinsed with DIW to remove trace levels of organics. Baseline monitoring of DIW after cleaning the system verified its cleanliness.

Epifluorescence microscopy was used to enumerate microbial cells in the water samples by concentrating 2-8 mL of water fixed with borate-buffered formalin onto black isopore filters, as described by Christner et al. (2018). A Nikon Eclipse Ni-E microscope was used to count the number of DNA-containing cells in 30 - 40 fields of view, which was used to estimate the cell concentration for each sample.

To estimate viable microbial biomass, ATP was quantified from cells concentrated on the filters and using the ATP Biomass Kit HS (Biothema, 266-311) following previously described methods (Christner et al., 2018). The relative luminescence units before and after addition of an internal standard (1 pmol of ATP) was used to calculate the concentration of ATP in each sample (Lundin, 2000). Chlorophyll *a* was extracted from filters using 90% v/v aqueous acetone as described by Welschmeyer (1994) and fluorescence was measured using a Qubit 3 fluorometer (Excitation: 470 nm; Emission 665 - 720 nm). Chlorophyll in biofilm samples (0.03 - 0.99 g) was also extracted in acetone and water soluble pigments were extracted in 50 mM sodium phosphate buffer pH 6.8 using a freeze-thaw method (Horváth et al., 2013). Chlorophyll-a was also measured on samples of glacier discharge and hot spring discharge soon using a ECO-FL-NTU(RT) Chlorophyll & Turbidity sensor (WET Labs Inc.) with a detection limit of 0.025 µg/L. Widefield fluorescence and brightfield microscopy were performed on live returned unstained samples using an Olympus IX71 inverted microscope with a 40x objective (numerical aperture of 0.7). Fluorescence emission was collected using Hg lamp excitation with a multiband filter set (Chroma multiband filter #89402, 391-32/479-33/554-24/638-31) captured on a Zeiss Axiocam 305 RGB camera. Data processing was performed using Zeiss Zen.

2.3 Data Analysis

End member mixing analysis was used to quantify the relative proportions of glacier discharge and hot spring discharge to Step Creek (equation 1 and 2). Bromide (Br^-), chloride (Cl^-) and fluoride (F^-) serve as effective tracers in this system according to the conditions specified by Barthodl et al (2011) since 1) they have extreme concentrations in the hot spring and glacier discharge (SI Table 1), 2) they are considered conservative in many aquatic systems because they do not tend to precipitate as salts, to interact with rocks along a stream channel, or to be significantly taken up by the biomass (Davis et al., 1998), 3) we expect concentrations in the source waters to have remained relatively constant over our sampling period because solute concentrations in discharge from glaciers without complex/dynamic subglacial drainage systems (as is the case for Crater Glacier; Walder et al., 2010) tend to remain stable towards the end of the melt season and Cl^- concentrations in hot spring discharge do not fluctuate dramatically over time (Bergfeld et al, 2008), and 4) we expect the solutes to be well mixed at our sampling site 2 km downstream (after a waterfall).

$$F_{Gl} = \frac{[HAL]_{DS} - [HAL]_{HS}}{[HAL]_{GL} - [HAL]_{HS}} \quad \text{(equation 1)}$$

$$1 = F_{GL} + F_{HS} \quad \text{(equation 2)}$$

Where F represents the fractional contribution, HS refers to hot spring discharge, GL refers to glacier discharge and DS refers to Mixed Downstream discharge. [HAL] represents the concentration of bromide, chloride or fluoride.

We then used the fractional contribution of the hot spring and glacier discharge from the end member mixing analysis to estimate the concentration of other biogeochemical parameters, assuming conservative mixing conditions (Equation 3).

$$[X]_{DS} = F_{GL}[X]_{GL} + F_{HS}[X]_{HS} \quad \text{(equation 3)}$$

Where [X] represents the concentration of other biogeochemical parameters in glacier discharge (GL), hot spring discharge (HS) and modeled downstream discharge (DS).

Model results assume conservative mixing conditions for biogeochemical parameter [X]. We therefore compare our observed [X] to modeled results to determine whether parameter X behaves conservatively, or whether there is a net source or sink for that parameter along Step Creek according to the following logic:

- We consider the analyte to have net source(s) if observed concentrations are greater than all three modeled concentrations: $[X]_{observed} > [X]_{modeled}$

- We consider the analyte to have net sink(s) if observed concentrations are less than all three modeled concentrations: $[X]_{observed} < [X]_{modeled}$

- We consider the analyte to behave conservatively, or have sinks that are in equilibrium with sources, if observed concentrations are not consistently greater than, or less than, all three modeled concentrations: $[X]_{observed} = [X]_{modeled}$

Mass spectra for SPE-DOM were calibrated using Predator Analysis software (Blakney et al., 2011) and molecular formulae were assigned with PetroOrg software (Corilo, 2015). SPE-DOM composition was summarized by: (1) molecular diversity (number of assigned formula); (2) heteroatomic content, as molecular formula containing only carbon, hydrogen, and oxygen (CHO), and formulae with nitrogen (CHON), sulfur (CHOS) or both nitrogen and sulfur (CHONS); (3) modified aromaticity index (AI_{mod}) (Koch & Dittmar, 2006); (4) Nominal oxidation state of carbon (NOSC) (Riedel et al., 2012); (5) the proportion of potentially chemically stable molecular formulae falling in the Island of Stability (Lechtenfeld et al., 2014); and (6) six formula categories which include condensed aromatics, polyphenolics, highly unsaturated and phenolic, aliphatic, peptide-like, and sugar-like following previous definitions (Kellerman et al., 2021; Osterholz et al., 2016; Spencer, et al., 2014b).

The partial pressure of CO_2 (pCO_2) was estimated for each water sample using pH and HCO_3^- concentrations following methods described by Raiswell and Thomas (1984). ATP concentration data for the three sample sites were used to estimate viable biomass with a conversion factor for aquatic systems proposed by Karl (1980):

$$B = 250\ x\ ATP \quad \text{(equation 4).}$$

Where B is biomass in grams of carbon (g C) and ATP is in grams of ATP (g ATP).

Spearman correlation coefficients were used to assess the monotonic association between cell numbers and biomass. Analysis of variance (ANOVA) was used to compare ATP and cell concentrations between samples.

3 Results

3.1 Glacier Discharge

Stream water, collected approximately 100 m from the terminus of Crater Glacier, was cold (0.7 °C), contained high suspended sediment concentrations (580 mg L^{-1}), was dilute (low total solutes; 12 mg L^{-1}), and had high pCO2 ($10^{-2.8}$ atm) compared to waters in equilibrium with the atmosphere ($10^{-3.4}$ atm). Solute was dominated by Si, Na^+, and HCO_3^-, with dissolved trace elements dominated by first series transition metals and lanthanide rare earth trace metals (Figure 2a and b), which were predominantly in the colloidal/nanoparticulate size fraction (SI Figure S1). The glacier discharge contained the highest NO_3^- concentrations (2.9 µM) and the lowest PO_4^{3-} (1.3 µM, Figure 2), DOC (7.5 µM), and FDOM fluorescence values measured in this study (Figure 3). The SPE-DOM had a high molecular diversity and contained a relatively high proportion of oxidized and aromatic compounds, predominantly CHO and CHON in composition (Figure 3d-i). Though the DOM in glacier discharge had the highest terrestrial DOM signatures of the samples explored in this study (e.g. abundance of polyphenolic and condensed aromatic formulae and chlorophyll-like fluorescence; Figure 3), the terrestrial DOM signatures in glacier discharge remain lower than those in other freshwater systems and glacial environments with sedimentary bedrock, developed soils and/or vegetative cover in the upstream catchment (Kellerman et al., 2021).

The cell concentration of glacier discharge based on epifluorescence microscopy was 3.4 ± 0.2 × 10^4 cells mL^{-1} and the concentration of ATP was 2.4 ± 0.2 × 10^{-4} pmol mL^{-1} (Figure 4). The strong correlation between cell concentration and ATP across the sampling sites (r_s=0.93, $p<0.05$, n=9) was used to derive cellular ATP content and estimate carbon biomass, resulting in concentrations of 7.2 ± 0.4 x 10^{-12} nmol $cell^{-1}$ and 30.8 ± 1.9 pg C mL^{-1}, respectively (Figure 4). Chlorophyll *a* (1.0 µg L^{-1}) (Figure 4) was the only chlorophyll detected, and it was only found in the water samples as no benthic biofilms or mats were present at this site. The few motile microorganisms observed in the glacier discharge were small (~1µm) and were therefore probably prokaryotes (Figure 5).

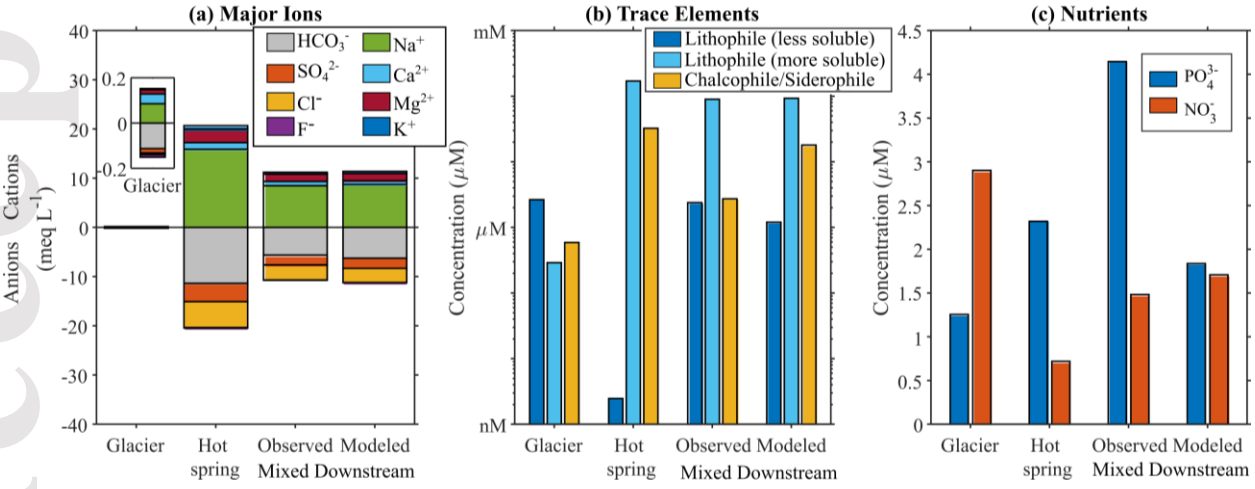

Figure 2: Geochemical summary of measurements of glacier, hot spring, and Mixed Downstream discharge and modeled geochemistry (i.e. assuming only conservative mixing) of Mixed Downstream discharge including (a) major anion and cation concentrations, (b) dissolved trace

element concentrations of 'less soluble' lithophiles (i.e. first series transition metals, actinides/lanthanides/Y - Al, Sc, Ti, V, Cr, Y, La, Ce, Pr, Nd and U), 'more soluble' lithophiles (alkali/alkaline earth elements – Li, Sr, Cs, and Ba) and chalcophiles/siderophiles (Mn, Mo, Co, Fe, Ni, Cd, Cu, and Pb), and (c) dissolved nutrient concentrations.

3.2 Hot Spring Discharge

The hot spring waters were warm (51.5 °C) and solute-rich (41.3 meq L^{-1}) and had high pCO_2 ($10^{-0.7}$ atm) compared to waters in equilibrium with the atmosphere ($10^{-3.4}$ atm). In-situ measurements of temperature and electrical conductivity along the upper reach of Step Creek identified five discrete hot spring seeps into Step Creek, all within a 35 m. No influxes of hot spring water into Step Creek were detected outside this area.

Solutes in hot spring discharge were dominated by Na^+, SO_4^{2-}, Cl^- and HCO_3^- and trace element composition was dominated by alkali/alkaline earth metals (Li, Sr, Cs, Ba) and to a lesser extent siderophiles /chalcophiles (Mn, Mo, Co, Fe, Ni, Cd, Cu). The hot spring waters contained 5-fold higher DOC concentrations (40.2 µM) than glacier discharge (Figure 3). Hot spring SPE-DOM had relatively low molecular diversity and mass, low AI_{mod}, and consisted of compounds with low NOSC and a high proportion of potentially stable compounds, i.e. those in the 'Island of Stability' (Lechtenfeld et al., 2014) (Figure 3). Although most SPE-DOM could be considered highly unsaturated and phenolic (%RA), there was a higher relative abundance of aliphatic, peptide-like and sulfur-containing compounds than in the glacier discharge SPE-DOM (Figure 3h; %RA). FDOM in the hot spring was predominantly protein-like and had the highest fluorescence per unit DOC among the environments measured in this study, suggesting a higher proportion of its DOC was fluorescent. However, most FDOM in the hot spring precipitated out of solution when the sample was left to settle for approximately 25 minutes (88%, 90% 82%, 67%, and 0% of the fluorescence at emission wavelengths 320, 340, 375, 500, and 675, respectively) (Figure 3b).

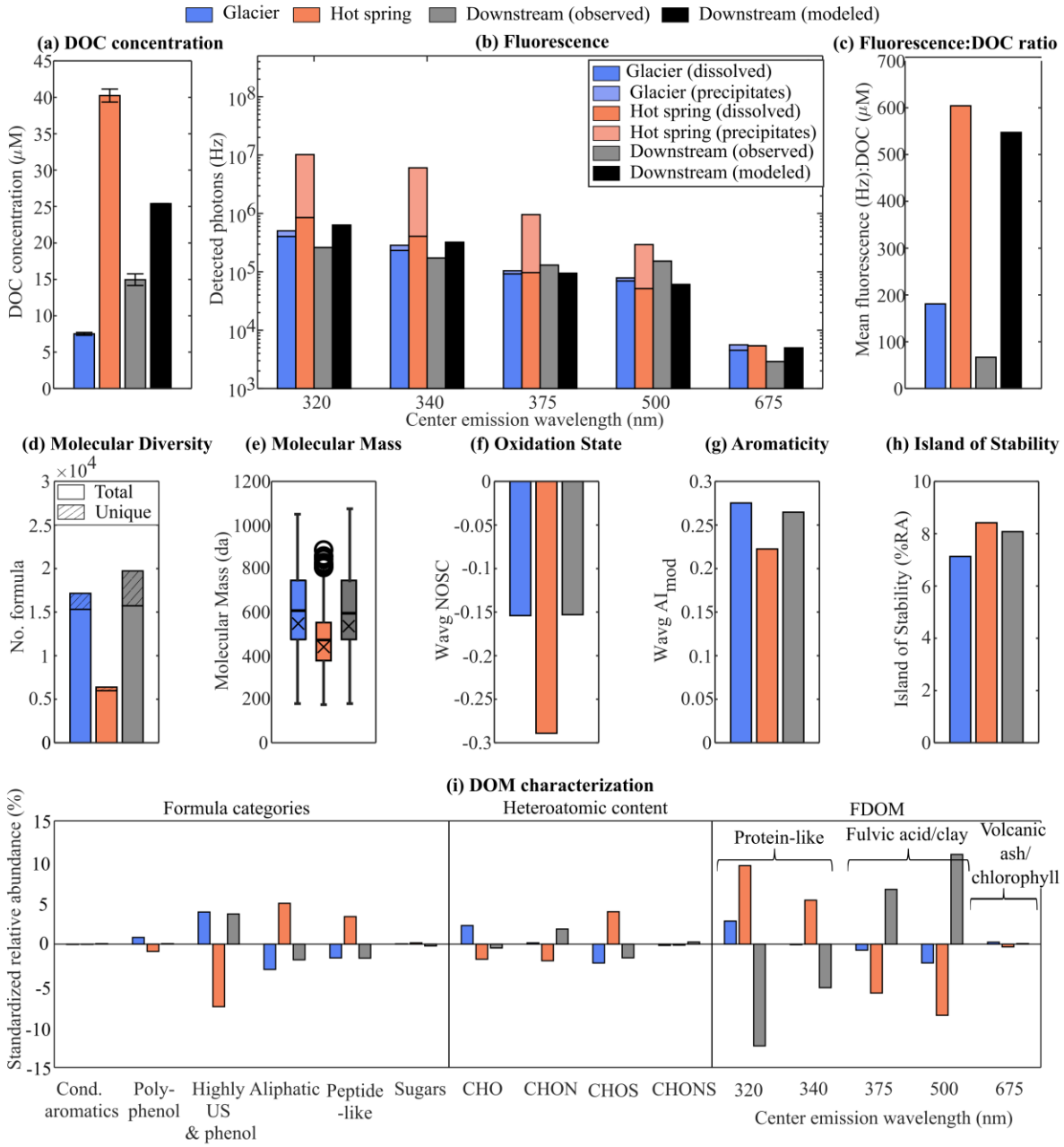

Figure 3: Summary of dissolved organic matter at the three sample sites including (a) DOC concentrations, (b) FDOM emission measurements (excitation wavelength = 255 nm), (c) mean fluorescence : DOC ratio, SPE-DOM (d) molecular diversity, (e) molecular mass (box plots display the median, the lower and upper quartiles, outliers defined by the interquartile range, and the minimum and maximum values that are not outliers; 'x' marks the weighted average), (f) the nominal oxidation state of carbon (Riedel et al., 2012), (g) modified aromaticity index (Koch & Dittmar, 2006), (h) relative abundance of molecules that are commonly considered stable

(Lechtenfeld et al., 2014), and (i) relative abundance of SPE-DOM (expressed by formula categories and heteroatomic content) and FDOM (expressed by emission intensity relative to the sum of emission intensities for all measured wavelengths) for each sample type. Note relative abundances are standardized by subtracting the relative abundance for each sample from the average relative abundance among glacier, hot spring and downstream samples for that DOM category. Parameters that represent concentration (a-c) include modeled concentrations for the Mixed Downstream site, but parameters derived from relative abundance data (d-i) do not. Colors represent glacier discharge (blue), hot spring discharge (orange), and Mixed Downstream (grey) unless indicated otherwise.

Cell concentration in the hot spring discharge ($8.8 \pm 0.7 \times 10^3$ cells mL^{-1}) was two-fold lower than that in the glacier discharge. Although the ATP concentration ($1.2 \pm 0.2 \times 10^{-4}$ pmol ATP mL^{-1}) and inferred carbon biomass (14.9 ± 2.6 pg C mL^{-1}) were about half of the concentrations observed in glacier discharge, the ATP content per cell was nearly twice that of the other samples ($1.3 \pm 0.3 \times 10^{-11}$ nmol ATP $cell^{-1}$), although these differences were not statistically significant (ANOVA, $p>0.05$, $n=3$) (Figure 4). Chlorophyll *a*, determined by in-field measurement, was low in the hot spring discharge (0.04 µg L^{-1}) (Figure 4) and no benthic mats or biofilms were visible.

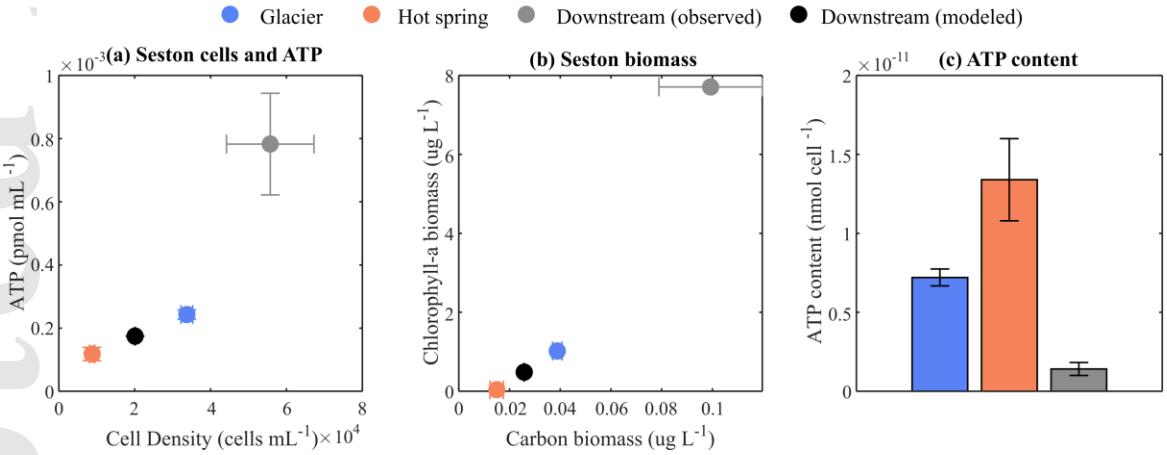

Figure 4: (a) ATP versus cell density, (b) Chlorophyll *a* versus carbon biomass estimated from ATP concentrations in water samples at the three samples sites, and (c) ATP content derived from data in (a). Error bars represent 1 standard deviation when replicate laboratory measurements were taken (for glacier, hot spring and Mixed Downstream (observed)) or the minimum and maximum modeled values (for downstream modeled). Note modeled concentrations assume conservative mixing conditions (Equation 3).

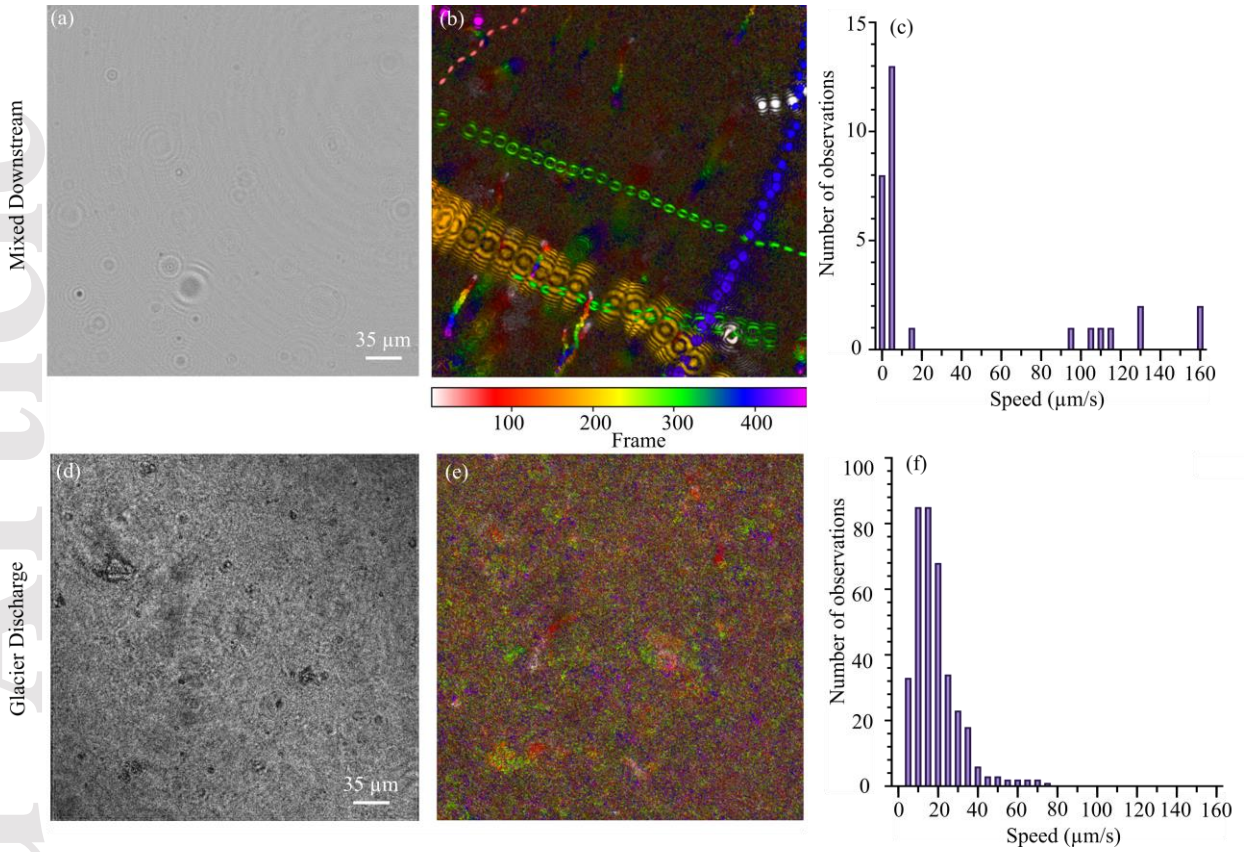

Figure 5: Images and corresponding particle speeds in untreated and unconcentrated water at the Mixed Downstream (top row) and glacier discharge (bottom row) sites captured via DHM. (a) and (d) are median-subtracted amplitude reconstructed hologram images (see supplementary Movies S1 and S2 showing motility). (b) and (e) are plots showing maximum pixel change at each time point of the holograms, collected at 15 frames/second for 32 seconds. (c) and (f) are histograms summarizing the speed of tracks identified in (b) and (e). Tracks identified from the software that are affiliated with large particles (>5 um in diameter) and speeds of >100 um/sec were confirmed by visual inspection to correspond to cells, whereas most tracks <100 um/sec could correspond to cells or debris. In some cases, more than one track may be assigned to a single cell (tracks were not stitched).

3.3 Mixed Waters (Upstream and Downstream)

Step Creek was cold (0.7 °C) and dilute (14 µS cm^{-1}) in the upper reach, but temperature and solutes rapidly increased in the vicinity of the hot springs, from 7.2 °C to 16.8 °C, and 9.6 µS cm^{-1} to 502 µS cm^{-1} (Figure 1b). Both temperature and conductivity showed strong gradients across the channel where the two water sources met (i.e., the Mixed Upstream sampling site). Benthic biofilms were observed at the Mixed Upstream sampling site, where the hot spring waters mix with glacier water, and the water temperature was 26 °C (Figure 1b, Figure 6a). Spectral analysis of pigments extracted from the benthic biofilms showed peaks for chlorophyll-a, carotenoids, and phycocyanin, indicated the presence of cyanobacteria (Figure 6c). No spectra characteristic of bacteriochlorophylls were detected, suggesting these biofilms unlikely contained anoxygenic phototrophic bacteria (Yurkov & Beatty, 1998). Fluorescence microscopy confirmed chlorophyll autofluorescence of the cyanobacteria and microminerals could be seen entangled in

the biofilms (Figure 6). Stationary cyanobacteria could also be identified in the DHM images by their dark color indicating the presence of chlorophyll (Figure 6e). A large number of motile organisms, with a variety of swimming speeds and sizes (1-20 µm) were present, but outside the focal plane of the biofilms (Figure 6e).

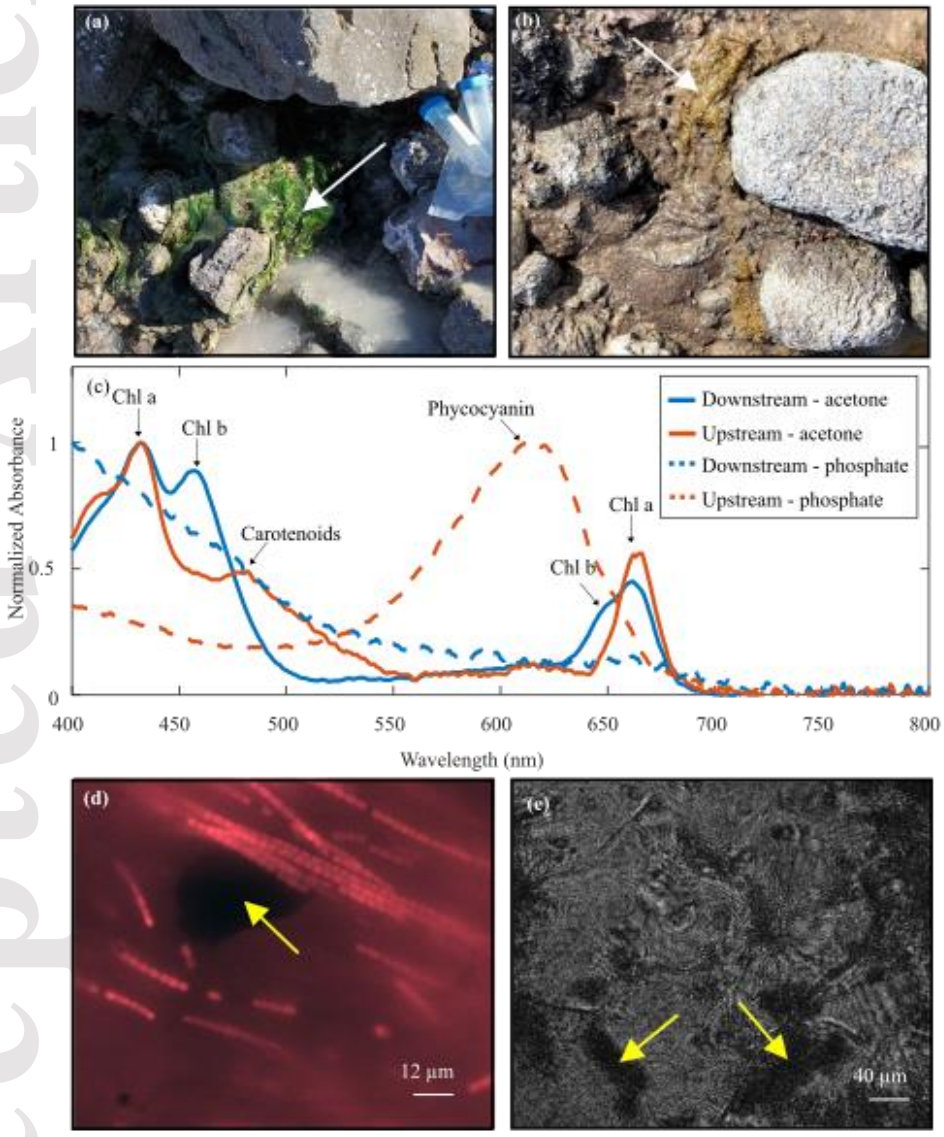

Figure 6: Benthic material at the Mixed Upstream (a) and downstream (b) sampling sites shown with arrows. Note 50 ml conical tube for scale in (a), with field of view in (b) at approximately the same scale as (a). (c) pigment concentrations for the material in (a) and (b). Pigments were extracted in either 90% acetone or 50 mM Na_3PO_4 as noted. (d) Images of benthic material at the Mixed Upstream sampling site using fluorescence microscopy with no stain (40x). (e) Amplitude reconstruction of a DHM image of the benthic material at a single focal plane (z=0) and time point for which a supplementary video is available (Movie S3) showing the presence of

organisms with range of swimming speeds, morphologies and sizes. Yellow arrows in (d) and (e) show sediment.

Approximately 2 km downstream of the confluence of the two water sources (i.e. at the 'Mixed Downstream' sampling site; Figure 1), conductivity increased to 973 µS cm^{-1} and water temperature was 13.9°C (Figure 1). Br^-, Cl^- and F^- mass balance calculations (equation 1 and 2) imply that water at the Mixed Downstream site was comprised of 51 - 58% hot spring water and 42 - 49% glacial meltwater at the time of sampling. Water chemistry was dominated by Na^+, HCO_3^- and Cl^-, with enrichment in Ca^{2+} (26 - 78 µM), Si (42 - 249 µM), and PO_4^{3-} (2.3 - 2.4 µM), and depletion in HCO_3^- (191 - 1090 µM), K^+ (23 - 86 µM), and NO_3^- (0.1 - 0.3 µM), compared to conservative behavior predicted by the mixing model (Figure 7). Dissolved trace elements were dominated by Alkali/Alkaline Earth metals (Figure 2), but the waters were consistently enriched (by 45 - 243%) in most of the 'less-soluble' lithophile elements (First Series Transition Metals/Lanthanides/Actinides, excluding Cr and Sc) and consistently depleted (by 7 - 95%) in siderophile /chalcophiles compared to predicted conservative behavior (Figure 7). Conservative mixing conditions suggest the hot spring supplied 5-8 times more DOC to Step Creek than did the glacier. The DOC concentration at the Mixed Downstream site was 14 µM (Figure 3), which is 38 - 44% (or ~6 µM) less than the conservative mixing model prediction (Figures 3 and 5), with more depleted FDOM at lower wavelengths (affiliated with protein-like material) than at higher wavelengths (affiliated with fulvic acids and chlorophyll) (Figure 7). Although the hot springs are estimated to contribute >5 times more DOC to Step Creek than the glacier, the SPE-DOM at the Mixed Downstream site was remarkably similar to the composition of SPE-DOM in the glacier discharge. Specifically, SPE-DOM at the Mixed Downstream site was similar to glacier SPE-DOM and distinct from hot spring SPE-DOM in terms of molecular diversity (n = 19,719 formula), molecular mass ($\bar{x}$ = 600 Da), oxidation state (NOSC=0.15), and aromaticity (AI_{mod}=0.26)(Figure 3 d-g). Like glacier discharge, most of the downstream SPE-DOM composition was categorized as highly unsaturated and phenolic compounds (85% RA), aliphatics (7% RA) and peptide-like (3% RA) (Figure 3i). However, discharge at the Mixed Downstream site had a higher proportion of N-containing SPE-DOM than either water source and, like the hot spring discharge, and had a higher relative abundance of potentially recalcitrant DOM (i.e. those in the 'Island of Stability'; Figure 3 h, i).

Biological signatures associated with seston at the Mixed Downstream site were higher than those in the glacier or hot spring discharge and those predicted by the conservative mixing model (ANOVA, $p > 0.05$; $n = 3$) (Figure 7). For instance, cell concentrations determined by epifluorescence microscopy ($5.6 \pm 1.2 \times 10^4$ cells mL^{-1}) were 104 - 132% higher than modeled, as were ATP ($7.8 \pm 1.6 \times 10^{-4}$ pmol ATP mL^{-1}), cellular ATP content ($1.4 \pm 0.4 \times 10^{-11}$ nmol $cell^{-1}$), carbon biomass (99.3 ± 20.0 pg C mL^{-1}) and chlorophyll-a (7.7 µg L^{-1}) (336 - 361%, 33 - 39%, 271 – 300 % and 1373 - 1632%, respectively; Figure 4, Figure 7). Motile eukaryotes and prokaryotes were associated with seston at the Mixed Downstream site (Figure 5; Movie S1). Spectral analysis of pigments extracted from benthic biofilms at the Mixed Downstream site showed peaks for Chl *a*, Chl *b*, and carotenoids, indicating the presence of green algae (Figure 6).

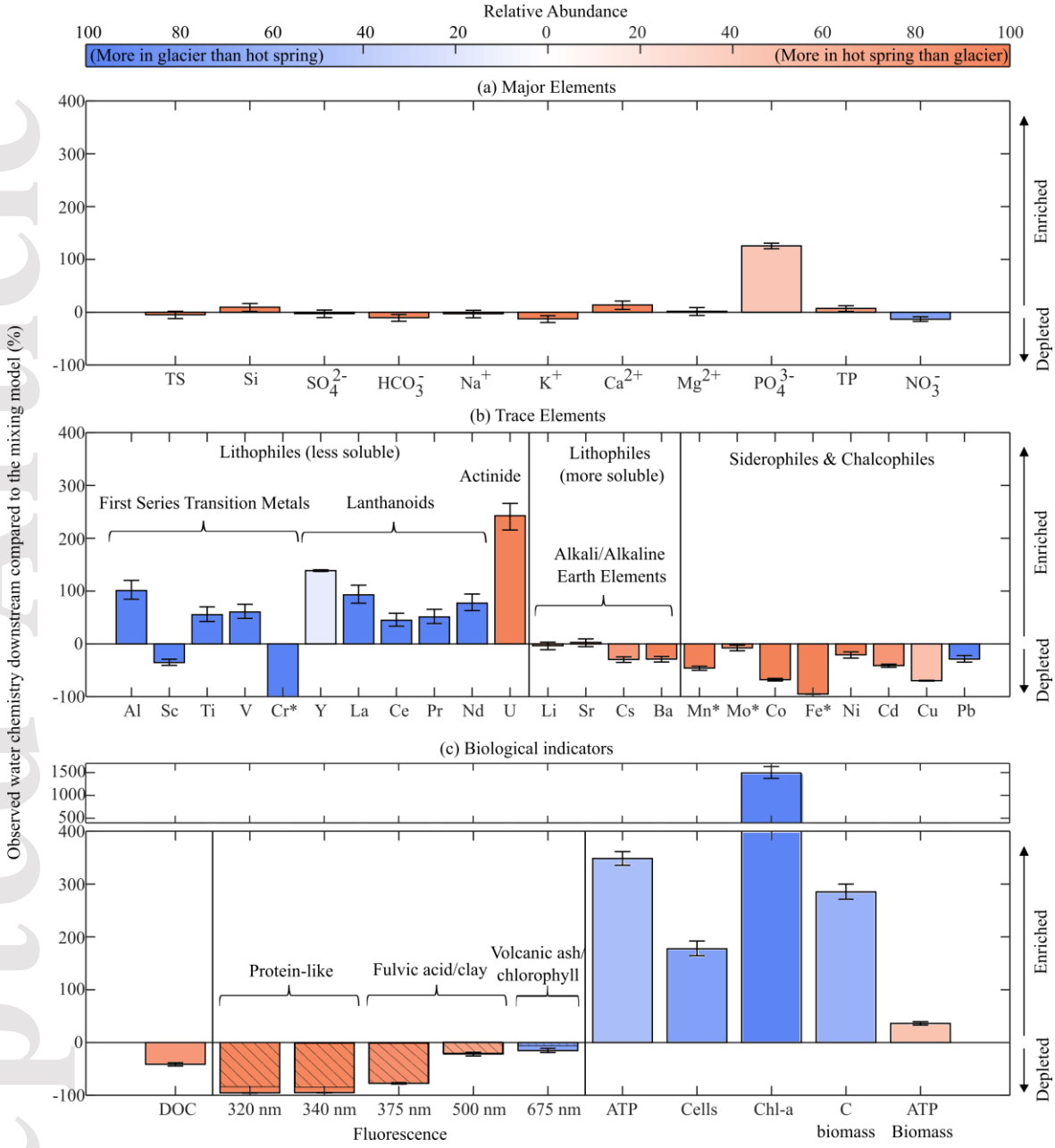

Figure 7: Difference between observed and modeled (assuming conservative mixing conditions) water chemistry at the Mixed Downstream sampling site calculated by: $\frac{[X]_{obs} - [X]_{modeled}}{[X]_{modeled}} \times 100$, where 'X' is the concentration of each chemical parameter for (a) total solutes (TS), major elements and total phosphorus (TP), (b) trace elements (<0.22 µM), and (c) biological indicators. Error bars indicate the variability in mixing models using Cl^-, Br^- and F^- as tracer elements (Equations 1-3). Hashed marks indicate the proportion of fluorescence that can be explained by precipitation and orange-blue colors indicate whether each parameter was relatively enriched in the hot spring discharge (orange) vs the glacier discharge (blue). For example, a blue bar indicates the parameter was more abundant in the glacier discharge compared to the hot spring discharge. The positive and negative bars indicate whether the parameter was enriched or

depleted at the Mixed Downstream mixed site compared to the mixing model. *Note Cr, Mo, Fe, and Mn can show both lithophile and siderophile characteristics.

4 Discussion

4.1. Water Sources

4.1.1 Glacier discharge

Previous studies suggest glacier meltwater rapidly drains from the surface to the bed of Crater Glacier due to the abundant crevassing, permeating a shallow subsurface aquifer that is comprised of a thick layer of coarse rock debris that produced in the 1980 avalanche and from pyroclastic deposits (Bedrosian et al., 2007; Walder et al., 2007). Since these waters transit through a relatively efficient drainage system (Walder et al., 2007), they probably remain oxic and capable of weathering the dacite that protrudes the glacier (Pallister et al., 2008) and the debris avalanche and pyroclastic deposits that underlie the glacier (Walder et al., 2007). The dissolved and colloidal material detected in glacier discharge comprises elements found in the Earth's crust that are acquired by erosion and/or weathering of silicate minerals. For example, glacier discharge contained relatively high concentrations of first series transition metals and lanthanoids, which are commonly derived from silicate weathering (Fleischer, 1954; Goldstein & Jacobsen, 1988; Hans Wedepohl, 1995; Shiller & Mao, 2000), including reactive pyroclastic material (Malpas et al., 2001; Marra & D'ambrosio, 2012). Cl^- and SO_4^{2-} content in surface waters are an indicator of contact with exsolved brines/the magmatic system at Mount St. Helens (Bergfeld et al., 2008; Shevenell & Goff, 1993) or sulfide oxidation in glacier systems (e.g. Anderson et al., 2000; Tranter et al., 2002), so their relatively low concentrations in glacier meltwater (Figure 2) imply that these waters remain isolated from the subsurface magmatic system and experience limited sulfide oxidation.

Though the glacially-derived solutes did not contain high concentrations of many inorganic nutrients (e.g. P, Fe, Mn, K, C, S) compared to the hot spring, these waters contained higher concentrations of inorganic nitrogen and unsaturated and phenolic organic compounds. Since silicate rocks do not contain high concentrations of NO_3^- or DOC, these components were probably derived from atmospheric deposition, though DOC could also have been produced by microbes on the ice surface (Spencer et al., 2014b; Stubbins et al., 2012). Concentrations of NO_3^- (2.9 µM) and DOC (7.5 µM) in glacier discharge were consistent with atmospheric deposition rates, and similar to, or less than, respective concentrations in other regional glaciers/snow field samples that overlie basaltic rocks (Fegel et al., 2016; Hamilton & Havig, 2016). The high relative abundance of unsaturated and phenolic compounds (84%) and protein-like fluorescence in glacier discharge (Figure 3) is also consistent with DOM from wet and dry atmospheric deposition or produced by autochthonous sources, as has been observed in other studies (Feng et al., 2018; Iavorivska et al., 2017; Kellerman et al., 2018, 2021). The DOM composition of glacier discharge has a relatively limited terrestrial signature (i.e. condensed aromatics and polyphenolics) compared to those in other freshwater systems and glacial environments with sedimentary bedrock, developed soils and/or vegetative cover in the upstream catchment (Kellerman et al., 2021; Spencer et al., 2014a; Stubbins et al., 2012).

Concentrations of cells and ATP biomass in glacier discharge were consistent with those reported in other glacial meltwaters (Barnett et al., 2016; Cameron et al., 2016; Sharp et al.,

1999; Takeuchi, 2001). The microbes released in glacier meltwater typically originate from the supraglacial and subglacial environment (Hodson et al., 2008), where near 0°C temperatures (Margesin et al., 2002) and low nutrient availability (Anesio & Laybourn-Parry, 2012) often limits metabolic activity. ATP serves as a proxy for viable biomass (Lundin et al., 1986), and the low ATP content per cell in glacier discharge relative to those at the Mixed Downstream site imply these cells are energy limited (Hammes et al., 2010) and/or comprised of dormant cells released to the supraglacial or subglacial environments.

4.1.2. Hot spring discharge

The hot springs in the Mount St. Helens crater drain a shallow aquifer that is recharged by precipitation and meltwater from Crater Glacier (Wynn et al., 2016). There is evidence that hot brines affiliated with this shallow aquifer exist near the boundary of the still-hot dacite intrusive rock (J. Wynn et al., 2016), and that water vapor is exsolved from deep cooling magma and condenses at shallower depths where it mixes with meteoric waters, some of which feeds the thermal springs in Loowit and Step Creeks (Bedrosian et al., 2007). The major and trace element composition of the hot spring discharge were consistent with waters that mix with exsolved brines from the magmatic system and weather fresh basalt rocks. Acidic gas species (i.e. CO_2, H_2S, SO_2, and/or HCl) are released from the magma (Bergfeld et al., 2017) and can react with minerals along the subsurface flow path to produce SO_4^{2-}, Cl^- and HCO_3^- (Bergfeld et al., 2008). Alkali/alkaline earth elements were found at high concentrations in the hot springs. These elements are highly soluble in aqueous fluids, tend to concentrate in exsolved brines and are preferentially weathered from rocks (Gaillardet et al., 1999; Nesbitt et al., 1980); they therefore likely originated from the magmatic system or freshly crystallized basaltic rocks.

High rates of mineral weathering and groundwater mixing with exsolved brines and/or magmatic gases produce highly reduced waters. In 2002 and 2005, Bergfeld et al. (2008) reported hot spring gas bubbles in Loowit Canyon to be dominated by CO_2 (76.3 - 80.2%) and N_2 (18.6 - 23.3%), while O_2 concentrations (5 ppb) were well below atmospheric equilibrium concentrations and reduced gas species (i.e. CH_4, H_2, H_2S) were detected (at concentrations of 0.05-0.06%, 0.0003% and 0.0026% respectively). Consistent with Bergfeld et al. (2017), we measured high concentrations of elemental species such as sFe (21 µM) and sMn (6.7 µM). Since their reduced species (i.e. Fe^{2+}, Mn^{2+}) are more soluble than their oxidized species (i.e. Fe^{3+}, Mn^{7+}), such high concentrations are typically only reached in waters with circumneutral pH when an oxidizing agent (O_2) is absent. We also measured low concentrations of oxidized species, such as NO_3^- (0.7 µM), compared to regional meteoric water (Hamilton & Havig, 2016) . NO_3^- has high reduction potential and can become depleted in reduced waters (i.e. those without O_2) where it often serves as an important electron acceptor.

The organic matter composition of the hot spring discharge possesses many features that are characteristic of geothermal systems. In addition to surface organic matter sources, hydrothermal waters can be exposed to subsurface, thermally-altered, sedimentary organic matter (Clifton et al., 1990; Des Marais et al., 1981; Retelletti Brogi et al., 2019; Rossel et al., 2017). At Mount St. Helens, the hot springs drain through pyrolyzed organic matter (from the pre-blast coniferous forest) that was deposited amongst the pyroclastic-flow deposits (Baross et al., 1982; Swanson & Major, 2005). These thermally-altered DOM sources could explain the 5-fold higher DOC concentrations observed in the hot spring compared to the glacier discharge (Figure 2), and concentrations that are an order of magnitude higher than those in regional alpine snow and ice

(Fegel et al., 2016; Hamilton & Havig, 2016). The high temperature and pressures of hydrothermal systems can degrade organic matter to gaseous end products (Hawkes et al., 2015; McCollom et al., 1999, 2001), resulting in DOM that have distinctive organic chemical characteristics. Thermally-altered DOM often has low molecular diversity and mass, consists of formula with low O/C ratios and AI_{mod}, but a high proportion of heteroatomic compounds, particularly those containing sulfur (Butturini et al., 2020; Hawkes et al., 2016; LaRowe et al., 2017; Longnecker et al., 2018; Rossel et al., 2017), as observed in hot spring discharge (Figure 3). FDOM is often a ubiquitous fraction of the DOM in hydrothermal fluids (Nye et al., 2020), since aromatic DOM is largely resistant to complete thermal degradation (McCollom et al., 1999, 2001).

Hydrothermal waters are often saturated with dissolved silicate. As the waters cool and flow towards the surface, silica precipitates as sinter along the subsurface conduits, effectively isolating these waters from the intrusion of oxidants from the surface environment (Gibson & Hinman, 2013; Vitale et al., 2008). The absence of light energy to fuel photosynthesis and oxidized electron acceptors to fuel chemotrophic microbial metabolisms most likely restricts microbial activity in these subsurface hydrothermal waters. Consistent with this theory, we measured low cell concentrations, biomass, and ATP compared to glacier discharge (Figure 4) suggesting limited microbial activity in the subsurface hydrothermal drainage system.

4.2. Mixed waters

The major ion and trace element geochemistry of the mixed waters in Step Creek was between that of the two water sources, and broadly similar to those predicted by the conservative mixing model (Figure 2). Major components of Step Creek biogeochemistry were therefore predominantly controlled by conservative mixing processes between the glacier and hot spring discharge. For example, Na^+, Mg^{2+}, and SO_4^{2-} were present at the Mixed Downstream site at concentrations within the range predicted by the conservative mixing model (Figure 7), suggesting they remain in solution as free ions, or that any potential in-stream sources are in equilibrium with sinks. Although conservative mixing processes define major aspects of the bulk chemistry of the downstream waters, many major ions deviated by small proportions (<15 %) compared to concentrations predicted by the conservative mixing model, while many trace elements, DOM categories, and biological signatures deviated by large proportions (-100% - 1400%) compared to concentrations predicted by the conservative mixing model (Figure 7). Systematic trends of enrichment or depletion among specific groups of solutes are consistent with in-stream biogeochemical processes that include 1) flocculation and the precipitation of Fe (oxy)hydroxides, 2) pH effects, and 3) the development of an in-stream ecosystem.

4.2.1. Flocculation and the precipitation of Fe (oxy)hydroxides

An orange precipitate was observed at the hot springs and along Step Creek, which is characteristic of freshly precipitated Fe (oxy)hydroxides that are widely known to occur at the redox boundaries of hot springs, and that have been described in nearby Loowit Canyon (Shevenell & Goff, 1993). Freshly precipitated Fe (oxy)hydroxides occur initially as poorly-crystalline nanomaterial with a comparatively large concentration of reactive hydroxyl (OH) groups (e.g. ferrihydrite) (Drits et al., 1993). As a consequence, freshly precipitated nanoparticulate aggregates have high adsorption capacities for many metals (Benjamin & Leckie, 1981) and DOM (Gentile et al., 2018). This adsorption capacity is even more prevalent during

the oxidation and co-precipitation of Mn^{2+} (Hochella et al., 2005). Since most siderophiles and chalcophiles, including Cr, Co, Ni, Cd, Cu, and Pb, have a low affinity for oxygen and preferentially bond with iron and sulfur they are commonly scavenged by iron (oxy)hydroxides (Benjamin & Leckie, 1981; Dai et al., 2017; Olivié-Lauquet et al., 2000; Regenspurg & Peiffer, 2005).

Two lines of evidence indicate the presence of an in-stream sink for a large fraction of the hot spring DOM. First, even though the hot spring supplied 5-8 times more DOC to Step Creek than did the glacier, the DOM in the mixed waters downstream had little resemblance to hot spring DOM and was instead remarkably similar to that from the glacier. Second, the mixed waters dowsntream had 38% lower DOC than would be the case if DOC mixed conservatively (Figure 3). Abiotic adsorption or co-precipitation of DOC with Fe (oxy)hydroxides has been observed at redox boundaries in many other environments (Linkhorst et al., 2017; Sholkovitz, 1976; Sinsabaugh et al., 1986), including hydrothermal systems (Gomez-Saez et al., 2015). However, most studies that have explored the DOM characteristics affiliated with Fe adsorption, have observed systematic coagulation of large (>450 Da), oxygen-rich and highly aromatic DOM molecules of terrestrial origin (Gomez-Saez et al., 2015; Linkhorst et al., 2017; Riedel et al., 2012). Compared to the hot spring discharge, the glacier discharge was characterized by larger, more oxygen-rich and aromatic DOM, with a greater terrestrial signature, so we would expect Fe-coagulation in the mixing zone to favor glacially-derived DOM over hot spring-derived DOM. Instead, the composition of DOM at the Mixed Downstream site inidicates the preferential removal of hot spring DOM. Fe-coagulation could preferentially remove hot spring DOM if the process occurred before the waters thoroughly mixed. Riedel et al., (Riedel et al., 2012) reported high rates of DOM removal with little fractionation at DOM/metal ratios similar to those in the hot spring (~1), so if Fe-coagulation occurred before the waters were thoroughly mixed, the process may indiscriminantly remove most hot spring-derived DOM. Alternatively, hot spring-derived DOM could be preferentially removed if it is largely hydrophobic. Hydrophobic DOM readily dissolves/stays in solution at high temperatures but not at lower temperatures (Reemtsma et al., 1999), so hydrophobic DOM would preferentially flocculate/precipitate when the hot spring waters (51.5 °C) mix with the glacier sourced discharge (7.2 °C).

4.2.2. pH effects

Both water sources (glacier and hot springs) had circumneutral pH (6.4-6.6), but the mixed, downstream waters had a pH of 9.0. While carbonate and/or silicate weathering along stream channels has resulted in high pH in other proglacial streams (e.g. Crompton et al., 2015; Hawkings et al., 2016; Wadham et al., 2000), this is unlikely the case in Step Creek since major ion concentrations and the ionic composition do not indicate high rates of in-stream weathering. Substantial in-stream biological drawdown of CO_2 (e.g. photosynthesis) is also unlikely to explain this rise in pH since such increases in pH are rare in non-eutrophic waterbodies. For example, Arctic and subarctic kelp forests, exposed to long photoperiods, in more poorly-buffered waters, are only capable of raising pH by fractions of a unit (Jensen et al., 2016). Instead, CO_2 gas-exchange could raise the pH of Step Creek since estimates of pCO_2 in both hot spring ($10^{-0.7}$ atm) and glacier ($10^{-2.8}$ atm) discharge suggest the source waters were super-saturated with respect to atmospheric CO_2, consistent with CO_2 measurements at Loowit hot springs (Bergfeld et al., 2017). In-stream CO_2 gas-exchange would reduce the pCO_2 and the

concentration of HCO_3^- in the stream water (Figure 7) and raise the pH. Further, gas-exchange would occur as the mixed waters flow over a 30 m tall waterfall before reaching the Mixed Downstream sampling site, where pCO2 was calculated to be near equilibrium with atmospheric concentrations. Although we do not have the measurements to verify or constrain the effects of CO_2 outgassing on raising pH, it would nevertheless play an important role with respect to the solubility and mobility of certain dissolved aqueous species.

Discharge at the Mixed Downstream site was enriched in dSi and dissolved trace elements compared to the conservative mixing model, including First Series Transition Metals, Lanthanides/Y and U, which are commonly associated with silicate minerals (Figure 7). High pH (>8) enhances the solubility of both primary aluminosilicate minerals and amorphous silica (Queneau & Berthold, 1986), so the increase in pH along Step Creek would facilitate the dissolution of these minerals. The downstream enrichment in lanthanides/Y/U was exclusively in the colloidal fraction (SI Figure S1) since they readily form complexes (Byrne et al., 1988; Elder, 1975) or attach to particle surfaces (Goldberg et al., 1963; Turner et al., 1981) including Fe/Mn (oxy)hydroxides (Haley et al., 2004; Sholkovitz et al., 1994), volcanic ash (e.g., Bagnato et al., 2013; Langmann, 2013; Varekamp et al., 1986), mineral dust (Erel et al., 2006; Marx et al., 2008) or clays (Cullers et al., 1975; Grandjean et al., 1987; Zhang et al., 2016). In contrast to the lanthanides/Y/U, Cs and Ba also form basic oxides, but because they are usually less abundant in silicate minerals, we expect their dissolved concentrations to decrease as the pH rises.

The increase in pH could also explain the notably higher U and PO_4^{3-} concentrations at the Mixed Downstream site compared to the conservative mixing model (Figure 7). These elements are the only elements analyzed that were at higher concentration in the hot spring water than the glacier water, and show among the highest relative enrichment downstream compared to the conservative mixing model (by 270% and 131%, respectively). Though U could be supplied by carbonate weathering along Step Creek, U and PO_4^{3-} adsorption to Fe(oxy)hydroxides is pH sensitive. U and PO_4^{3-} adsorb onto Fe(oxy)hydroxides in neutral waters (e.g. hot spring and glacier meltwater), but desorb at high pH when Fe (oxy)hydroxides reach their point of zero charge (Aiuppa et al., 2000), as would be the case downstream (pH=9). We hypothesize the desorption of negatively charged U and P species from the surface of Fe (oxy)hydroxides resulted in the high relative enrichment of these elements observed downstream compared to the conservative mixing model (Figure 7, Figure S1).

4.2.3. In-stream ecosystem

The seston communities in the mixed waters downstream contained higher concentrations of microbial cells and biomass (i.e. ATP and Chlorophyll *a*) than either of the water sources, (Figure 4). Unlike the water sources, the mixed waters also contained a diverse range of motile eukarytotes with diverse morphologies and sizes and supported biofilms and eukaryotic algae (Figure 5). Together, these biological indicators suggest the mixed waters supported a more productive ecosystem than either water source.

Mixing of the two distinct water sources could promote biological activity by introducing chemical disequilibrium that could fuel chemotrophic microbial metabolisms. Previous studies of a volcanic subglacial lake and glacially-influenced volcanic lakes have found molecular evidence for chemotrophic bacteria that utilize the redox gradient between geothermal and glacial water sources by using iron, sulfide, sulfur or hydrogen (common geothermal components) as electron donors and oxygen, sulfate, nitrate or carbon dioxide (common glacier components) as electron

acceptors (Gaidos et al., 2009; Moreras- Marti et al., 2021). The glacier discharge we sampled was cold (0.7 °C) and contained a relative abundance of compounds that are common in oxidized waters (e.g. NO_3^-, O_2) but few compounds that are common in reduced waters (e.g. sFe, sMn) while the opposite was observed in the warm (51.5 °C) hot spring discharge. The mixing of these two water sources could therefore supply chemical energy sources from which microbes could fuel their metabolisms, in water temperatures more suitable to a wide range of organisms (Podar et al., 2020).

Mixing of the two distinct water sources could also promote biological activity by providing a comprehensive suite of nutrients. Glacier discharge contained relatively high concentrations of dissolved inorganic nitrogen, whereas the hot spring contained relatively high concentrations of other dissolved macro- and micro-nutrients including PO_4^{3-}, Fe, Mn, and DOM. Once mixed, these waters could stimulate the growth of exogenous microbes, aerotolerant microbes from the hot spring, or the nutrient-limited cells from the glacial melt (Facey et al., 2019; Kohler et al., 2016). In turn, this microbial activity would deplete concentrations of dissolved nutrients downstream (Figure 7; except PO_4^{3-} which is controlled by abiotic processes as discussed above). Heterotrophic microbial activity, through DOC utilization could also contribute to the lower DOC concentrations at the Mixed Downstream sample site (Figure 7). Among fractions of FDOM, heterotrophic microbes are known to preferentially utilize protein-like material (e.g. Coble, 2014; Fox et al., 2017, 2018), which was among the most depleted components in the mixed waters downstream (Figure 3b; Figure 7).

Although benthic communities were not evident in either of the water sources, widespread biofilms were established within 1 m of the initial mixing zone in Step Creek, providing strong evidence that biological activity is enhanced in the mixing zone. Biofilms at the Mixed Upstream site were found to contain cyanobacteria based on the presence of phycocyanin as well as microscopic images showing filamentous organisms (Figure 6). Cyanobacteria are often among the first organisms to colonize environments, particularly those with conditions too extreme for microalgae to exist, since they can survive in a range of water temperatures and types, including hot springs (Dadheech et al., 2013) and glacier ice (Chrismas et al., 2015; Kvíderová et al., 2018). Biofilms at the Mixed Downstream site contained both chlorophyll a and b, which is characteristic of green algae (Jeffrey et al., 1997). These organisms can play important roles in the cycling and storage of nutrients because they fix CO_2, uptake nitrate (Baker et al., 2009; Herrero et al., 2001; Makhalanyane et al., 2015) and produce material that can maintain redox gradients for other ecological niches (Van Goethem & Cowan, 2019). The development of the benthic community in the mixed waters is coincident with a more diverse pool of SPE-DOM, including numerous SPE-DOM compounds that were present in the mixed waters downstream but were absent in either of the water sources (Figure 3c). These unique SPE-DOM compounds could indicate autochthonous DOM production, since seston and benthic communities can produce a diverse range of DOM molecules (Fiore et al., 2015; Kujawinski, 2010; Kujawinski et al., 2009; Noriega-Ortega et al., 2019) by passive diffusion across the cell membrane or by active exudation into the surrounding environment.

5 Conclusions

We characterized the nutrients, chemical energy sources, and biomass associated with hot spring and glacier discharge within the crater of Mount St. Helens and evaluated the biogeochemical evolution of these waters after they mixed in Step Creek. Glacier meltwater and

hot spring discharge contained different concentrations and compositions of major ions, trace elements, and dissolved organic matter (DOM). The hot spring contained comparatively high concentrations of biogeochemically-reactive components (e.g. many siderophile and chalcophile trace elements and DOM), but a large fraction of these components were depleted in Step Creek once the waters mixed, effectively diminishing the downstream biogeochemical signature of the hot spring. In contrast, glacier discharge contained less solute, largely derived from atmospheric deposition and silicate weathering within the glacial catchment, but the geochemical signatures contained in glacier discharge largely persisted after the waters mixed in Step Creek. The mixing of glacier and hot spring water in Step Creek supported higher seston and benthic biomass than those in either of the two water sources. This suggests the mixing environment promotes ecosystem development, perhaps through utilization of the redox gradient established which in turn contributes to nutrient and DOM cycling. Conservative mixing processes do play a role in defining downstream biogeochemistry. However, Fe (oxy)hydroxide precipitation, changes in pH as geothermal waters degas, and the increasing complexity and biomass of seston and benthic ecosystems are likely key processes controlling the concentration and speciation of the reactive components of the system. Though the composition of hot springs and glacier discharge can vary between systems, these findings advance our understanding of biogeochemical processes that can occur at the interface between volcanic and cryospheric systems, which are widespread on Earth. There may also be broader relevance since the interaction between volcanic and cryospheric systems on other planetary bodies have been identified as potential sites to host extraterrestrial life.

Author Contributions

Conceptualization: AD, QF, MS, NB, BC, PD, JN, CS

Investigation, Review and editing: all authors

Funding acquisition: MS, NB, BC, PD, JN

Formal analysis and writing – original draft: AD, QF

Acknowledgments, Samples, and Data

This research was supported by a NASA PSTAR grant (80NSSC18K1738) for THOR (Thermal High-voltage Ocean-penetrator Research platform). Partial support was also provided (to B.C.C. and Q.F.) by a grant from the National Science Foundation (OPP-2000649) and the University of Florida's Water Institute Graduate Fellowship program. A portion of this work was performed at the National High Magnetic Field Laboratory ICR User Facility, which is supported by the National Science Foundation Division of Chemistry and Division of Materials Research through DMR-1644779 and the State of Florida. We thank the Mount St. Helens National Volcanic Monument for permission to access and sample in the crater and the Mount St. Helens Institute for permission to establish a field camp. We thank Stone Aerospace and Vickie Siegel for field camp logistics and field assistance and Kathryn Bywaters for assistance with sample collection. Data supporting the conclusions of this paper are available from the Open Science Framework Repository (FI-ICR mass spectral files; DOI 10.17605/OSF.IO/PRKN9) and Zenodo (10.5281/zenodo.7102401).

References

Aiuppa, A., Allard, P., D'Alessandro, W., Michel, A., Francesco Parello, M. T., & Valenza, M. (2000). Mobility and fluxes of major, minor and trace metals during basalt weathering and groundwater transport at Mt. Etna volcano (Sicily). *Geochmica et Cosmochimica Acta*, *64*(11), 1827–1841. https://doi.org/10.1038/sj.bdj.4804658

Anderson, S. P., Drever, J. I., Frost, C. D., & Holden, P. (2000). Chemical weathering in the foreland of a retreating glacier. *Geochimica et Cosmochimica Acta*, *64*(7), 1173–1189. https://doi.org/10.1016/S0016-7037(99)00358-0

Anesio, A. M., & Laybourn-Parry, J. (2012). Glaciers and ice sheets as a biome. *Trends in Ecology & Evolution*, *27*(4), 219–225. https://doi.org/10.1016/j.tree.2011.09.012

Bagnato, E., Aiuppa, A., Bertagnini, A., Bonadonna, C., Cioni, R., Pistolesi, M., et al. (2013). Scavenging of sulphur, halogens and trace metals by volcanic ash: The 2010 Eyjafjallajökull eruption. *Geochimica et Cosmochimica Acta*, *103*, 138–160. https://doi.org/10.1016/j.gca.2012.10.048

Baker, M. A., Guzman, G. De, & Ostermiller, J. D. (2009). Differences in nitrate uptake among benthic algal assemblages in a mountain stream. *Journal of the North American Benthological Society*, *28*(1), 24–33. https://doi.org/10.1899/07-129.1

Barnett, M. J., Pawlett, M., Wadham, J. L., Jackson, M., & Cullen, D. C. (2016). Demonstration of a multi-technique approach to assess glacial microbial populations in the field. *Journal of Glaciology*, *62*(232), 348–358. https://doi.org/10.1017/jog.2016.23

Baross, J. A., Dahm, C. N., Ward, A. K., Lilley, M. D., & Sedell, J. R. (1982). Initial microbiological response in lakes to the Mt St Helens eruption. *Nature*, *296*(5852), 49–52. https://doi.org/10.1038/296049a0

Bedrosian, P. A., Unsworth, M. J., & Johnston, M. J. S. (2007). Hydrothermal circulation at Mount St. Helens determined by self-potential measurements. *Journal of Volcanology and Geothermal Research*, *160*(1–2), 137–146. https://doi.org/10.1016/j.jvolgeores.2006.09.003

Bedrossian, M., Wallace, J. K., Serabyn, E., Lindensmith, C., & Nadeau, J. (2020). Enhancing final image contrast in off-axis digital holography using residual fringes. *Optics Express*, *28*(11), 16764–16771. https://doi.org/10.1364/OE.394231

Benjamin, M. M., & Leckie, J. O. (1981). Multiple-site adsorption of Cd, Cu, Zn, and Pb on amorphous iron oxyhydroxide. *Journal of Colloid and Interface Science*, *79*(1), 209–221. https://doi.org/10.1016/0021-9797(81)90063-1

Bergfeld, D., Evans, W. C., McGee, K. A., & Spicer, K. R. (2008). Pre- and post-eruptive investigations of gas and water samples from Mount St. Helens, Washington, 2002 to 2005. *US Geological Survey Professional Paper*, (1750), 523–542. https://doi.org/10.3133/pp175025

Bergfeld, D., Evans, W. C., Spicer, K. R., Hunt, A. G., & Kelly, P. J. (2017). Evidence for degassing of fresh magma during the 2004–2008 eruption of Mount St. Helens: Subtle signals from the hydrothermal system. *Journal of Volcanology and Geothermal Research*, *343*, 109–121. https://doi.org/10.1016/j.jvolgeores.2017.06.020

Björnsson, H. (2002). Subglacial lakes and jökulhlaups in Iceland. *Global Planet. Change*, *35*,

255–271.

Bramall, N. E. (2007). *The remote sensing of microorganisms*. *PhD thesis*. University of California, Berkeley.

Burns, R., Wynn, P. M., Barker, P., McNamara, N., Oakley, S., Ostle, N., et al. (2018). Direct isotopic evidence of biogenic methane production and efflux from beneath a temperate glacier. *Scientific Reports*, *8*(1), 1–8. https://doi.org/10.1038/s41598-018-35253-2

Butturini, A., Amalfitano, S., Herzsprung, P., Lechtenfeld, O. J., Venturi, S., Olaka, L. A., et al. (2020). Dissolved Organic Matter in Continental Hydro-Geothermal Systems: Insights from Two Hot Springs of the East African Rift Valley. *Water*, *12*(12), 3512. https://doi.org/10.3390/w12123512

Byrne, R. H., Kump, L. R., & Cantrell, K. J. (1988). The influence of temperature and pH on trace metal speciation in seawater. *Marine Chemistry*, *25*(2), 163–181. https://doi.org/10.1016/0304-4203(88)90062-X

Cameron, K. A., Stibal, M., Hawkings, J. R., Mikkelsen, A. B., Telling, J. P., Kohler, T. J., et al. (2016). Meltwater export of prokaryotic cells from the Greenland Ice Sheet. *Environmental Microbiology*, *19*(2), 524–534. https://doi.org/10.1111/1462-2920.

Chrismas, N. A. M., Anesio, A. M., & Sánchez-Baracaldo, P. (2015). Multiple adaptations to polar and alpine environments within cyanobacteria: a phylogenomic and Bayesian approach. *Frontiers in Microbiology*, *6*, 1070. https://doi.org/10.3389/FMICB.2015.01070

Christiansen, R. L., & Peterson, D. W. (1981). *Chronology of the 1980 eruptive activity. U.S. Geological Survey Professional Paper 1250*.

Christner, B. C., Lavender, H. F., Davis, C. L., Oliver, E. E., Neuhaus, S. U., Myers, K. F., et al. (2018). Microbial processes in the weathering crust aquifer of a temperate glacier. *The Cryosphere*, *12*(11), 3653–3669. https://doi.org/10.5194/tc-12-3653-2018

Clark, E. B., Bramall, N. E., Christner, B. C., Flesher, C., Harman, J., Hogan, B., et al. (2018). An intelligent algorithm for autonomous scientific sampling with the VALKYRIE cryobot. *International Journal of Astrobiology*, *17*(3), 247–257. https://doi.org/10.1017/S1473550417000313

Clifton, C. G., Walters, C. C., & Simoneit, B. R. T. (1990). Hydrothermal petroleums from Yellowstone National Park, Wyoming, U.S.A. *Applied Geochemistry*, *5*(1–2), 169–191. https://doi.org/10.1016/0883-2927(90)90047-9

Coble, P. G. (2014). *Aquatic organic matter fluorescence*. Cambridge: Cambridge University Press. https://doi.org/10.1017/CBO9781139045452

Cohoe, D., Hanczarek, I., Wallace, J. K., & Nadeau, J. (2019). Multiwavelength Digital Holographic Imaging and Phase Unwrapping of Protozoa Using Custom Fiji Plug-ins. *Frontiers in Physics*, *7*, 94. https://doi.org/10.3389/fphy.2019.00094

Corilo, Y. (2015). EnviroOrg. Florida State University.

Crompton, J. W., Flowers, G. E., Kirste, D., Hagedorn, B., Sharp, M. J., Hagedorn, B., & Sharp, M. J. (2015). Clay mineral precipitation and low silica in glacier meltwaters explored through reaction-path modelling. *Journal of Glaciology*, *61*(230), 1061–1078.

https://doi.org/10.3189/2015JoG15J051

Cullers, R. L., Chaudhuri, S., Arnold, B., Lee, M., & Wolf, C. W. (1975). Rare earth distributions in clay minerals and in the clay-sized fraction of the Lower Permian Havensville and Eskridge shales of Kansas and Oklahoma. *Geochimica et Cosmochimica Acta*, *39*(12), 1691–1703. https://doi.org/10.1016/0016-7037(75)90090-3

Curtis, A., & Kyle, P. (2017). Methods for mapping and monitoring global glaciovolcanism. *Journal of Volcanology and Geothermal Research*, *333–334*, 134–144. https://doi.org/10.1016/j.jvolgeores.2017.01.017

Dadheech, P. K., Glöckner, G., Casper, P., Kotut, K., Mazzoni, C. J., Mbedi, S., & Krienitz, L. (2013). Cyanobacterial diversity in the hot spring, pelagic and benthic habitats of a tropical soda lake. *FEMS Microbiology Ecology*, *85*(2), 389–401. https://doi.org/10.1111/1574-6941.12128

Dai, C., Lin, M., & Hu, Y. (2017). Heterogeneous Ni- and Cd-Bearing Ferrihydrite Precipitation and Recrystallization on Quartz under Acidic pH Condition. *ACS Earth and Space Chemistry*, *1*(10), 621–628. https://doi.org/10.1021/acsearthspacechem.7b00097

Dartnell, L. R., Storrie-Lombardi, M. C., & Ward, J. M. (2010). Complete fluorescent fingerprints of extremophilic and photosynthetic microbes. *International Journal of Astrobiology*, *9*(4), 245–257. https://doi.org/10.1017/S1473550410000224

Davis, S. N., Whittemore, D. O., & Fabryka-Martin, J. (1998). Uses of Chloride/Bromide Ratios in Studies of Potable Water. *Groundwater*, *36*(2), 338–350. https://doi.org/10.1111/J.1745-6584.1998.TB01099.X

Drits, V. A., Sakharov, B. A., Salyn, A. L., & Manceau, A. A. (1993). Structural model for ferrihydrite. *Clay Minerals*, *28*, 185–207.

Elder, J. F. (1975). Complexation side reactions involving trace metals in natural water systems1. *Limnology and Oceanography*, *20*(1), 96–102. https://doi.org/10.4319/lo.1975.20.1.0096

Erel, Y., Dayan, U., Rabi, R., Rudich, Y., & Stein, M. (2006). Trans boundary transport of pollutants by atmospheric mineral dust. *Environmental Science and Technology*, *40*(9), 2996–3005. https://doi.org/10.1021/es051502l

Eshelman, E. J., Malaska, M. J., Manatt, K. S., Doloboff, I. J., Wanger, G., Willis, M. C., et al. (2019). WATSON: In Situ Organic Detection in Subsurface Ice Using Deep-UV Fluorescence Spectroscopy. *Astrobiology*, *19*(6), 771–784. https://doi.org/10.1089/AST.2018.1925

Facey, J. A., Apte, S. C., & Mitrovic, S. M. (2019). A review of the effect of trace metals on freshwater cyanobacterial growth and toxin production. *Toxins*, *11*(11). https://doi.org/10.3390/toxins11110643

Fegel, T. S., Baron, J. S., Fountain, A. G., Johnson, G. F., & Hall, E. K. (2016). The differing biogeochemical and microbial signatures of glaciers and rock glaciers. *Journal of Geophysical Research G: Biogeosciences*, *121*(3), 919–932. https://doi.org/10.1002/2015JG003236

Feng, L., An, Y., Xu, J., & Kang, S. (2018). Characteristics and sources of dissolved organic matter in a glacier in the northern Tibetan Plateau: Differences between different snow

categories. *Annals of Glaciology*, *59*(77), 31–40. https://doi.org/10.1017/aog.2018.20

Fiore, C., Longnecker, K., Kido Soule, M., & Kujawinski, E. (2015). Release of ecologically relevant metabolites by the cyanobacterium Synechococcus elongates CCMP 1631. *Environmental Microbiology*, *17*(10), 3949–3963. https://doi.org/10.1111/1462-2920.12899

Fleischer, M. (1954). The abundance and distribution of the chemical elements in the earth's crust. *Journal of Chemical Education*, *31*(9), 446–455. https://doi.org/10.1021/ed031p446

Fox, B. G., Thorn, R. M. S., Anesio, A. M., & Reynolds, D. M. (2017). The in situ bacterial production of fluorescent organic matter; an investigation at a species level. *Water Research*, *125*, 350–359. https://doi.org/10.1016/J.WATRES.2017.08.040

Fox, Bethany G., Thorn, R. M. S., Anesio, A. M., Cox, T., Attridge, J. W., & Reynolds, D. M. (2018). Microbial processing and production of aquatic fluorescent organic matter in a model freshwater system. *Water (Switzerland)*, *11*(1). https://doi.org/10.3390/W11010010

Fraser, C. I., Terauds, A., Smellie, J., Convey, P., & Chown, S. L. (2014). Geothermal activity helps life survive glacial cycles. *Proceedings of the National Academy of Sciences of the United States of America*, *111*(15), 5634–5639. https://doi.org/10.1073/pnas.1321437111

Fregoso, S. (2020). DHMx Software Suite. Retrieved from https://github.com/dhm-org/dhm_suite

Gabrielli, S., Spagnolo, M., & De Siena, L. (2020). Geomorphology and surface geology of Mount St. Helens volcano. *Journal of Maps*, *16*(2), 585–594. https://doi.org/10.1080/17445647.2020.1790048

Gaidos, E. J., Lanoil, B., Thorsteinsson, T., Graham, A., Skidmore, M. L., Han, S.-K., et al. (2004). A viable microbial community in a subglacial volcanic crater lake, Iceland. *Astrobiology*, *4*(3), 327–344. https://doi.org/10.1089/ast.2004.4.327

Gaidos, E. J., Marteinsson, V., Thorsteinsson, T., Jóhannesson, T., Rúnarsson, A. R., Stefansson, A., et al. (2009). An oligarchic microbial assemblage in the anoxic bottom waters of a volcanic subglacial lake. *The ISME Journal*, *3*(4), 486–97. https://doi.org/10.1038/ismej.2008.124

Gaillardet, J., Dupre, B., Louvat, P., & Allegre, C. J. (1999). Global silicate weathering and CO2 consumption rates deduced from the chemistry of large rivers. *Chemical Geology*, *159*, 3–30.

Garcia-Lopez, E., & Cid, C. (2017). Glaciers and ice sheets as analog environments of potentially habitable icy worlds. *Frontiers in Microbiology*, *8*, 1407. https://doi.org/10.3389/fmicb.2017.01407

Gentile, L., Wang, T., Tunlid, A., Olsson, U., & Persson, P. (2018). Ferrihydrite Nanoparticle Aggregation Induced by Dissolved Organic Matter. *The Journal of Physical Chemistry A*, *122*(38), 7730–7738. https://doi.org/10.1021/ACS.JPCA.8B05622

Gibson, M. L., & Hinman, N. W. (2013). Mixing of hydrothermal water and groundwater near hot springs, Yellowstone National Park (USA): hydrology and geochemistry. *Hydrogeology Journal*, *21*(4), 919–933. https://doi.org/10.1007/s10040-013-0965-4

Glicken, H. (1996). Rockslide-debris avalanche of may 18, 1980, Mount St. Helens volcano,

Washington. *Open-File Report 96-677*, 1–5.

Van Goethem, M. W., & Cowan, D. A. (2019). Role of Cyanobacteria in the Ecology of Polar Environments. In S. Castro-Sowinski (Ed.), *The Ecological Role of Micro-organisms in the Antarctic Environment* (pp. 2–23). Springer, Cham. https://doi.org/10.1007/978-3-030-02786-5_1

Goff, F., & McMurtry, G. M. (2000). Tritium and stable isotopes of magmatic waters. *Journal of Volcanology and Geothermal Research*, *97*(1–4), 347–396. https://doi.org/10.1016/S0377-0273(99)00177-8

Goldberg, E. D., Koide, M., Schmitt, R. A., & Smith, R. H. (1963). Rare-Earth distributions in the marine environment. *Journal of Geophysical Research*, *68*(14), 4209–4217. https://doi.org/10.1029/JZ068i014p04209

Goldstein, S. J., & Jacobsen, S. B. (1988). Rare earth elements in river waters. *Earth and Planetary Science Letters*, *89*, 35–47. https://doi.org/10.1016/0012-821X(88)90031-3

Gomez-Saez, G. V., Riedel, T., Niggemann, J., Pichler, T., Dittmar, T., & Bühring, S. I. (2015). Interaction between iron and dissolved organic matter in a marine shallow hydrothermal system off Dominica Island (Lesser Antilles). *Marine Chemistry*, *177*, 677–686. https://doi.org/10.1016/j.marchem.2015.10.003

Grandjean, P., Cappetta, H., Michard, A., & Albarède, F. (1987). The assessment of REE patterns and 143Nd144Nd ratios in fish remains. *Earth and Planetary Science Letters*, *84*(2–3), 181–196. https://doi.org/10.1016/0012-821X(87)90084-7

Haley, B. A., Klinkhammer, G. P., & McManus, J. (2004). Rare earth elements in pore waters of marine sediments. *Geochimica et Cosmochimica Acta*, *68*(6), 1265–1279. https://doi.org/10.1016/j.gca.2003.09.012

Hamilton, T. L., & Havig, J. (2016). Primary productivity of snow algae communities on stratovolcanoes of the Pacific Northwest. *Geobiology*, *15*(2), 280–295. https://doi.org/10.1111/gbi.12219

Hammes, F., Goldschmidt, F., Vital, M., Wang, Y., & Egli, T. (2010). Measurement and interpretation of microbial adenosine tri-phosphate (ATP) in aquatic environments. *Water Research*, *44*(13), 3915–3923. https://doi.org/10.1016/j.watres.2010.04.015

Hans Wedepohl, K. (1995). The composition of the continental crust. *Geochimica et Cosmochimica Acta*, *59*(7), 1217–1232. https://doi.org/10.1016/0016-7037(95)00038-2

Havig, J. R., & Hamilton, T. L. (2019). Snow algae drive productivity and weathering at volcanic rock-hosted glaciers. *Geochimica et Cosmochimica Acta*, *247*, 220–242. https://doi.org/10.1016/j.gca.2018.12.024

Hawkes, J. A., Rossel, P. E., Stubbins, A., Butterfield, D., Connelly, D. P., Achterberg, E. P., et al. (2015). Efficient removal of recalcitrant deep-ocean dissolved organic matter during hydrothermal circulation. *Nature Geoscience*, *8*(11), 856–860. https://doi.org/10.1038/ngeo2543

Hawkes, J. A., Hansen, C. T., Goldhammer, T., Bach, W., & Dittmar, T. (2016). Molecular alteration of marine dissolved organic matter under experimental hydrothermal conditions. *Geochimica et Cosmochimica Acta*, *175*, 68–85. https://doi.org/10.1016/j.gca.2015.11.025

Hawkings, J. R., Wadham, J. L., Tranter, M., Telling, J. P., Bagshaw, E. A., Beaton, A., et al. (2016). The Greenland Ice Sheet as a hotspot of phosphorus weathering and export in the Arctic. *Global Biogeochemical Cycles*, *30*, 1–22. https://doi.org/10.1002/2015GB005237

Hawkings, J. R., Skidmore, M. L., Wadham, J. L., Priscu, J. C., Morton, P. L., Hatton, J. E., et al. (2020). Enhanced trace element mobilization by Earth's ice sheets. *Proceedings of the National Academy of Sciences of the United States of America*, *117*(50), 31648–31659. https://doi.org/10.1073/pnas.2014378117

Hendrickson, C. L., Quinn, J. P., Kaiser, N. K., Smith, D. F., Blakney, G. T., Chen, T., et al. (2015). 21 Tesla Fourier Transform Ion Cyclotron Resonance Mass Spectrometer: A National Resource for Ultrahigh Resolution Mass Analysis. *Journal of The American Society for Mass Spectrometry*, *26*(9), 1626–1632. https://doi.org/10.1007/S13361-015-1182-2

Herrero, A., Muro-Pastor, A. M., & Flores, E. (2001). Nitrogen control in cyanobacteria. *Journal of Bacteriology*. https://doi.org/10.1128/JB.183.2.411-425.2001

Hochella, M. F., Kasama, T., Putnis, A., Putnis, C. V., & Moore, J. N. (2005). Environmentally important, poorly crystalline Fe/Mn hydrous oxides: Ferrihydrite and a possibly new vernadite-like mineral from the Clark Fork River Superfund Complex. *American Mineralogist*, *90*(4), 718–724. https://doi.org/10.2138/am.2005.1591

Hodson, A. J., Anesio, A. M., Tranter, M., Fountain, A., Osborn, M., Priscu, J. C., et al. (2008). Glacial Ecosystems. *Ecological Monographs*, *78*(1), 41–67. https://doi.org/10.1890/07-0187.1

Horváth, H., Kovács, A. W., Riddick, C., & Présing, M. (2013). Extraction methods for phycocyanin determination in freshwater filamentous cyanobacteria and their application in a shallow lake. *European Journal of Phycology*, *48*(3), 278–286. https://doi.org/10.1080/09670262.2013.821525

Iavorivska, L., Boyer, E. W., & Grimm, J. W. (2017). Wet atmospheric deposition of organic carbon: An underreported source of carbon to watersheds in the northeastern United States. *Journal of Geophysical Research*, *122*(5), 3104–3115. https://doi.org/10.1002/2016JD026027

Jeffrey, S. W., Mantoura, R. F. C., & Wright, S. W. (Eds.). (1997). *Phytoplankton pigments in oceanography: guidelines to modern methods. Monographs on oceanographic methodology; 10*. Paris: UNESCO Publishing.

Karl, D. M. (1980). Cellular Nucleotide Measurements and Applications in Microbial Ecology. *Microbiological Reviews*, *44*(4), 739–796.

Kellerman, A. M., Guillemette, F., Podgorski, D. C., Aiken, G. R., Butler, K. D., & Spencer, R. G. M. (2018). Unifying Concepts Linking Dissolved Organic Matter Composition to Persistence in Aquatic Ecosystems. *Environmental Science and Technology*, *52*(5), 2538–2548. https://doi.org/10.1021/acs.est.7b05513

Kellerman, A. M., Vonk, J., McColaugh, S., Podgorski, D. C., van Winden, E., Hawkings, J. R., et al. (2021). Molecular Signatures of Glacial Dissolved Organic Matter from Svalbard and Greenland. *Global Biogeochemical Cycles*, *35*(3). https://doi.org/10.1029/2020GB006709

Koch, B. P., & Dittmar, T. (2006). From mass to structure: An aromaticity index for high-resolution mass data of natural organic matter. *Rapid Communications in Mass Spectrometry*, *20*(5), 926–932. https://doi.org/10.1002/rcm.2386

Kohler, T. J., Horn, D. J. Van, Darling, J. P., Takacs-Vesbach, C. D., & McKnight, D. M. (2016). Nutrient treatments alter microbial mat colonization in two glacial meltwater streams from the McMurdo Dry Valleys, Antarctica. *FEMS Microbiology Ecology*, *92*(4). https://doi.org/10.1093/femsec/fiw049

Kujawinski, E. B. (2010). The Impact of Microbial Metabolism on Marine Dissolved Organic Matter. *Annual Review of Marine Science*, *3*, 567–599. https://doi.org/10.1146/ANNUREV-MARINE-120308-081003

Kujawinski, E. B., Longnecker, K., Blough, N. V., Vecchio, R. Del, Finlay, L., Kitner, J. B., & Giovannoni, S. J. (2009). Identification of possible source markers in marine dissolved organic matter using ultrahigh resolution mass spectrometry. *Geochimica et Cosmochimica Acta*, *73*(15), 4384–4399. https://doi.org/10.1016/J.GCA.2009.04.033

Kvíderová, J., Elster, J., & Komárek, J. (2018). Ecophysiology of Cyanobacteria in the Polar Regions. *Cyanobacteria: From Basic Science to Applications*. Elsevier. https://doi.org/10.1016/B978-0-12-814667-5.00014-3

Langmann, B. (2013). Volcanic Ash versus Mineral Dust: Atmospheric Processing and Environmental and Climate Impacts. *ISRN Atmospheric Sciences*, *2013*(Article ID 245076), 1–17. https://doi.org/10.1155/2013/245076

LaRowe, D. E., Koch, B. P., Robador, A., Witt, M., Ksionzek, K., & Amend, J. P. (2017). Identification of organic compounds in ocean basement fluids. *Organic Geochemistry*, *113*, 124–127. https://doi.org/10.1016/j.orggeochem.2017.07.017

Lechtenfeld, O. J., Kattner, G., Flerus, R., McCallister, S. L., Schmitt-Kopplin, P., & Koch, B. P. (2014). Molecular transformation and degradation of refractory dissolved organic matter in the Atlantic and Southern Ocean. *Geochimica et Cosmochimica Acta*, *126*, 321–337. https://doi.org/10.1016/J.GCA.2013.11.009

Linkhorst, A., Dittmar, T., & Waska, H. (2017). Molecular Fractionation of Dissolved Organic Matter in a Shallow Subterranean Estuary: The Role of the Iron Curtain. *Environmental Science and Technology*, *51*(3), 1312–1320. https://doi.org/10.1021/acs.est.6b03608

Longnecker, K., Sievert, S. M., Sylva, S. P., Seewald, J. S., & Kujawinski, E. B. (2018). Dissolved organic carbon compounds in deep-sea hydrothermal vent fluids from the East Pacific Rise at 9°50′N. *Organic Geochemistry*, *125*, 41–49. https://doi.org/10.1016/j.orggeochem.2018.08.004

Lundin, A. (2000). Use of firefly luciferase in atp-related assays of biomass, enzymes, and metabolites. In *Bioluminescence and Chemiluminescence Part C* (Vol. 305, pp. 346–370). Academic Press. https://doi.org/https://doi.org/10.1016/S0076-6879(00)05499-9

Lundin, A., Hasenson, M., Persson, J., & Pousette, A. (1986). Estimation of Biomass in Growing Cell Lines by Adenosine Triphosphate Assay. *Methods in Enzymology*, *133*(1983), 27–42.

Major, J. J., & Newhall, C. G. (1989). Snow and ice perturbation during historical volcanic eruptions and the formation of lahars and floods - A global review. *Bulletin of Volcanology*,

52(1), 1–27. https://doi.org/10.1007/BF00641384

Makhalanyane, T. P., Valverde, A., Velázquez, D., Gunnigle, E., Goethem, M. W. Van, Quesada, A., & Cowan, D. A. (2015). Ecology and biogeochemistry of cyanobacteria in soils, permafrost, aquatic and cryptic polar habitats. *Biodiversity and Conservation*. Kluwer Academic Publishers. https://doi.org/10.1007/s10531-015-0902-z

Malpas, J., Duzgoren-Aydin, N. S., & Aydin, A. (2001). Behaviour of chemical elements during weathering of pyroclastic rocks, Hong Kong. *Environment International*, *26*(5–6), 359–368. https://doi.org/10.1016/S0160-4120(01)00013-7

Des Marais, D. J., Donchin, J. H., Nehring, N. L., & Truesdell, A. H. (1981). Molecular carbon isotopic evidence for the origin of geothermal hydrocarbons. *Nature*, *292*(5826), 826–828. https://doi.org/10.1038/292826a0

Margesin, R., Zacke, G., & Schinner, F. (2002). Characterization of heterotrophic microorganisms in alpine glacier cryoconite. *Arctic, Antarctic, and Alpine Research*, *34*(1), 88–93. https://doi.org/10.2307/1552512

Marra, F., & D'ambrosio, E. (2012). Trace element classification diagrams of pyroclastic rocks from the volcanic districts of central Italy: the case study of the ancient Roman ships of Pisa. *Archaeometry*, *55*(6), 993–1019. https://doi.org/10.1111/j.1475-4754.2012.00725.x

Martinez-Alonso, E., Pena-Perez, S., Serrano, S., Garcia-Lopez, E., Alcazar, A., & Cid, C. (2019). Taxonomic and functional characterization of a microbial community from a volcanic englacial ecosystem in Deception Island, Antarctica. *Scientific Reports*, *9*(1), 1–14. https://doi.org/10.1038/s41598-019-47994-9

Marx, S. K., Kamber, B. S., & McGowan, H. A. (2008). Scavenging of atmospheric trace metal pollutants by mineral dusts: Inter-regional transport of Australian trace metal pollution to New Zealand. *Atmospheric Environment*, *42*(10), 2460–2478. https://doi.org/10.1016/j.atmosenv.2007.12.014

McCollom, T. M., Ritter, G., & Simoneit, B. R. T. (1999). Lipid synthesis under hydrothermal conditions by Fischer-Tropsch-type reactions. *Origins of Life and Evolution of the Biosphere*, *29*(2), 153–166. https://doi.org/10.1023/A:1006592502746

McCollom, T. M., Seewald, J. S., & Simoneit, B. R. T. (2001). Reactivity of monocyclic aromatic compounds under hydrothermal conditions. *Geochimica et Cosmochimica Acta*, *65*(3), 455–468. https://doi.org/10.1016/S0016-7037(00)00533-0

Moreras- Marti, A., Fox- Powell, M., Zerkle, A. L., Stueeken, E., Gazquez, F., Brand, H. E. A., et al. (2021). Volcanic controls on the microbial habitability of Mars- analogue hydrothermal environments. *Geobiology*, *19*(5), 489–509. https://doi.org/10.1111/gbi.12459

Mosbrucker, A. R. (2014). *High-resolution digital elevation model of Mount St. Helens crater and upper North Fork Toutle River basin, Washington, based on an airborne lidar survey of September 2009. Data Series 904, U.S. Geological Survey*. Reston, VA. https://doi.org/10.3133/ds904

Nesbitt, H. W., Markovics, G., & Price, R. C. (1980). Chemical processes affecting alkalis and alkaline earths during continental weathering. *Geochimica et Cosmochimica Acta*, *44*(11), 1659–1666. https://doi.org/10.1016/0016-7037(80)90218-5

Neukum, G., Jaumann, R., Hoffmann, H., Hauber, E., Head, J. W., Basilevsky, A. T., et al. (2004). Recent and episodic volcanic and glacial activity on Mars revealed by the High Resolution Stereo Camera. *Nature*, *432*(23/30), 971–979.

Noriega-Ortega, B. E., Wienhausen, G., Mentges, A., Dittmar, T., Simon, M., & Niggemann, J. (2019). Does the Chemodiversity of Bacterial Exometabolomes Sustain the Chemodiversity of Marine Dissolved Organic Matter? *Frontiers in Microbiology*, *10*, 215. https://doi.org/10.3389/FMICB.2019.00215

Nye, J. J., Shock, E. L., & Hartnett, H. E. (2020). A novel PARAFAC model for continental hot springs reveals unique dissolved organic carbon compositions. *Organic Geochemistry*, *141*, 103964. https://doi.org/10.1016/j.orggeochem.2019.103964

Olivié-Lauquet, G., Allard, T., Bertaux, J., & Muller, J. P. (2000). Crystal chemistry of suspended matter in a tropical hydrosystem, Nyong basin (Cameroon, Africa). *Chemical Geology*, *170*(1–4), 113–131. https://doi.org/10.1016/S0009-2541(99)00244-2

Orosei, R., Lauro, S. E., Pettinelli, E., Cicchetti, A., Coradini, M., Cosciotti, B., et al. (2018). Radar evidence of subglacial liquid water on Mars. *Science*, *361*(6401), 490–493. https://doi.org/10.1126/science.aar7268

Osterholz, H., Kirchman, D. L., Niggemann, J., & Dittmar, T. (2016). Environmental Drivers of Dissolved Organic Matter Molecular Composition in the Delaware Estuary. *Frontiers in Earth Science*, *4*, 95. https://doi.org/10.3389/FEART.2016.00095

Pallister, J. S., Thornber, C. R., Cashman, K. V., Clynne, M. A., Lowers, H. A., Mandeville, C. W., et al. (2008). Petrology of the 2004-2006 Mount St. Helens lava dome-implications for magmatic plumbing and eruption triggering. *US Geological Survey Professional Paper*, (1750), 647–702.

Pierson, T. C., Janda, R. J., Thouret, J. C., & Borrero, C. A. (1990). Perturbation and melting of snow and ice by the 13 November 1985 eruption of Nevado del Ruiz, Colombia, and consequent mobilization, flow and deposition of lahars. *Journal of Volcanology and Geothermal Research*, *41*(1–4), 17–66. https://doi.org/10.1016/0377-0273(90)90082-Q

Podar, P. T., Yang, Z., Björnsdóttir, S. H., & Podar, M. (2020). Comparative Analysis of Microbial Diversity Across Temperature Gradients in Hot Springs From Yellowstone and Iceland. *Frontiers in Microbiology*, *11*, 1625. https://doi.org/10.3389/FMICB.2020.01625

Price, P. B., Rohde, R. A., & Bay, R. C. (2009). Fluxes of microbes, organic aerosols, dust, sea-salt Na ions, non-sea-salt Ca ions, and methanesulfonate onto Greenland and Antarctic ice. *Biogeosciences*, *6*(3), 479–486. https://doi.org/10.5194/BG-6-479-2009

Price, S. F., & Walder, J. S. (2007). Modeling the dynamic response of a crater glacier to lava-dome emplacement: Mount St Helens, Washington, USA. *Annals of Glaciology*, *45*, 21–28. https://doi.org/10.3189/172756407782282525

Queneau, P. B., & Berthold, C. E. (1986). Silica in Hydrometallurgy: An Overview. *Canadian Metallurgical Quarterly*, *25*(3), 201–209. https://doi.org/10.1179/CMQ.1986.25.3.201

Reemtsma, T., Bredow, A., & Gehring, M. (1999). The nature and kinetics of organic matter release from soil by salt solutions. *European Journal of Soil Science*, *50*(1), 53–64. https://doi.org/10.1046/j.1365-2389.1999.00212.x

Regenspurg, S., & Peiffer, S. (2005). Arsenate and chromate incorporation in schwertmannite. *Applied Geochemistry*, *20*(6), 1226–1239. https://doi.org/10.1016/j.apgeochem.2004.12.002

Retelletti Brogi, S., Kim, J. H., Ryu, J. S., Jin, Y. K., Lee, Y. K., & Hur, J. (2019). Exploring sediment porewater dissolved organic matter (DOM) in a mud volcano: Clues of a thermogenic DOM source from fluorescence spectroscopy. *Marine Chemistry*, *211*, 15–24. https://doi.org/10.1016/j.marchem.2019.03.009

Riedel, T., Biester, H., & Dittmar, T. (2012). Molecular fractionation of dissolved organic matter with metal salts. *Environmental Science and Technology*, *46*(8), 4419–4426. https://doi.org/10.1021/es203901u

Rossel, P. E., Stubbins, A., Rebling, T., Koschinsky, A., Hawkes, J. A., & Dittmar, T. (2017). Thermally altered marine dissolved organic matter in hydrothermal fluids. *Organic Geochemistry*, *110*, 73–86. https://doi.org/10.1016/j.orggeochem.2017.05.003

Scanlon, K. E., Head, J. W., Wilson, L., & Marchant, D. R. (2014). Volcano-ice interactions in the Arsia Mons tropical mountain glacier deposits. *Icarus*, *237*, 315–339. https://doi.org/10.1016/j.icarus.2014.04.024

Schulze-Makuch, D., Dohm, J. M., Fan, C., Fairén, A. G., Rodriguez, J. A. P., Baker, V. R., & Fink, W. (2007). Exploration of hydrothermal targets on Mars. *Icarus*, *189*(2), 308–324. https://doi.org/10.1016/j.icarus.2007.02.007

Sharp, M. J., Parkes, J., Cragg, B., Fairchild, I. J., Lamb, H., & Tranter, M. (1999). Widespread bacterial populations at glacier beds and their relationship to rock weathering and carbon cycling. *Geology*, *27*(2), 107–110. https://doi.org/10.1130/0091-7613(1999)027<0107:WBPAGB>2.3.CO;2

Shevenell, L., & Goff, F. (1993). Addition of magmatic volatiles into the hot spring waters of loowit canyon, Mount St. Helens, Washington, USA. *Bulletin of Volcanology*, *55*(7), 489–503. https://doi.org/10.1007/BF00304592

Shiller, A. M., & Mao, L. (2000). Dissolved vanadium in rivers: Effects of silicate weathering. *Chemical Geology*, *165*(1–2), 13–22. https://doi.org/10.1016/S0009-2541(99)00160-6

Sholkovitz, E. R. (1976). Flocculation of dissolved organic and inorganic matter during the mixing of river water and seawater. *Geochimica et Cosmochimica Acta*, *40*(7), 831–845. https://doi.org/10.1016/0016-7037(76)90035-1

Sholkovitz, Edward R., Landing, W. M., & Lewis, B. L. (1994). Ocean particle chemistry: The fractionation of rare earth elements between suspended particles and seawater. *Geochimica et Cosmochimica Acta*, *58*(6), 1567–1579. https://doi.org/10.1016/0016-7037(94)90559-2

Sinsabaugh, R. L., Hoehn, R. C., Knocke, W. R., & Linkins, A. E. (1986). Removal of Dissolved Organic Carbon by Coagulation With Iron Sulfate. *Journal - American Water Works Association*, *78*(5), 74–82. https://doi.org/10.1002/j.1551-8833.1986.tb05747.x

Smith, H. J., Dieser, M., McKnight, D. M., SanClements, M. D., & Foreman, C. M. (2018). Relationship between dissolved organic matter quality and microbial community composition across polar glacial environments. *FEMS Microbiology Ecology ·*, (May), 1–10. https://doi.org/10.1093/femsec/fiy090

Spencer, R. G. M., Vermilyea, A., Fellman, J., Raymond, P., Stubbins, A., Scott, D., & Hood, E.

W. (2014a). Seasonal variability of organic matter composition in an Alaskan glacier outflow: insights into glacier carbon sources. *Environmental Research Letters*, *9*(5), 055005. https://doi.org/10.1088/1748-9326/9/5/055005

Spencer, R. G. M., Guo, W., Raymond, P. A., Dittmar, T., Hood, E. W., Fellman, J., & Stubbins, A. (2014b). Source and biolability of ancient dissolved organic matter in glacier and lake ecosystems on the Tibetan Plateau. *Geochimica et Cosmochimica Acta*, *142*, 64–74. https://doi.org/10.1016/j.gca.2014.08.006

Stubbins, A., Hood, E. W., Raymond, P. A., Aiken, G. R., Sleighter, R. L., Hernes, P. J., et al. (2012). Anthropogenic aerosols as a source of ancient dissolved organic matter in glaciers. *Nature Geoscience*, *5*(3), 198–201. https://doi.org/10.1038/ngeo1403

Swanson, F. J., & Major, J. J. (2005). Physical Events, Environments, and Geological—Ecological Interactions at Mount St. Helens: March 1980–2004. In *Ecological Responses to the 1980 Eruption of Mount St. Helens* (pp. 27–44). https://doi.org/10.1007/0-387-28150-9_3

Takeuchi, N. (2001). The altitudinal distribution of snow algae on an Alaska glacier (Gulkana Glacier in the Alaska Range). *Hydrological Processes*, *15*(18), 3447–3459. https://doi.org/10.1002/hyp.1040

Thompson, J. M. (1990). *Chemical data from thermal and nonthermal springs in Mount St. Helens National Monument, Washington*. *Open-File Report, U.S. Geological Survey*. https://doi.org/10.3133/ofr90690C

Tomasson, H. (1996). The jökulhlaup from Katla in 1918. *Annals of Glaciology*, *22*, 249–254. https://doi.org/10.1017/s0260305500015494

Tranter, M., Sharp, M. J., Lamb, H. R., Brown, G. H., Hubbard, B. P., & Willis, I. C. (2002). Geochemical weathering at the bed of Haut Glacier d'Arolla, Switzerland - a new model. *Hydrological Processes*, *16*(5), 959–993. https://doi.org/10.1002/hyp.309

Turner, D. R., Whitfield, M., & Dickson, A. G. (1981). The equilibrium speciation of dissolved components in freshwater and sea water at 25°C and 1 atm pressure. *Geochimica et Cosmochimica Acta*, *45*(6), 855–881. https://doi.org/10.1016/0016-7037(81)90115-0

Varekamp, J. C., Thomas, E., Germani, M., & Buseck, P. R. (1986). Particle geochemistry of volcanic plumes of Etna and Mount St. Helens. *Journal of Geophysical Research: Solid Earth*, *91*(B12), 12233–12248. https://doi.org/10.1029/JB091iB12p12233

Vitale, M. V., Gardner, P., & Hinman, N. W. (2008). Surface water-groundwater interaction and chemistry in a mineral-armored hydrothermal outflow channel, Yellowstone National Park, USA. *Hydrogeology Journal*, *16*(7), 1381–1393. https://doi.org/10.1007/s10040-008-0344-8

De Vries, M. V. W., Bingham, R. G., & Hein, A. S. (2018). A new volcanic province: An inventory of subglacial volcanoes in West Antarctica. *Geological Society Special Publication*, *461*(1), 231–248. https://doi.org/10.1144/SP461.7

Wadham, J. L., Tranter, M., & Dowdeswell, J. A. (2000). Hydrochemistry of meltwaters draining a polythermal-based, high-Arctic glacier, south Svalbard: II. Winter and early Spring. *Hydrological Processes*, *14*(10), 1767–1786. https://doi.org/10.1002/1099-

1085(200007)14:10<1767::AID-HYP103>3.0.CO;2-Q

Walder, J. S., LaHusen, R. G., Vallance, J. W., & Schilling, S. P. (2007). Emplacement of a silicic lava dome through a crater glacier: Mount St Helens, 2004-06. *Annals of Glaciology*, *45*, 14–20. https://doi.org/10.3189/172756407782282426

Walder, J. S., Schilling, S. P., Sherrod, D. R., & Vallance, J. W. (2010). Evolution of Crater Glacier, Mount St. Helens, Washington, September 2006-November 2009. *Open-File Report*, (November 2009).

Wallace, J. K., Rider, S., Serabyn, E., Lindensmith, C., & Nadeau, J. (2016). A Common-Mode Architecture for a Digital Holographic Microscope. In *Imaging and Applied Optics 2016* (p. DTh3F.2). Heidelberg: Optical Society of America. https://doi.org/10.1364/DH.2016.DTh3F.2

Wanke, M., Clynne, M. A., von Quadt, A., Vennemann, T. W., & Bachmann, O. (2019). Geochemical and petrological diversity of mafic magmas from Mount St. Helens. *Contributions to Mineralogy and Petrology*, *174*(1), 1–25. https://doi.org/10.1007/s00410-018-1544-4

Welschmeyer, N. A. (1994). Fluorometric analysis of chlorophyll a in the presence of chlorophyll b and pheopigments. *Limnology and Oceanography*, *39*(8), 1985–1992. https://doi.org/https://doi.org/10.4319/lo.1994.39.8.1985

Wynn, J., Mosbrucker, A., Pierce, H., & Spicer, K. (2016). Where is the hot rock and where is the ground water - Using CSAMT to map beneath and around Mount St. Helens. *Journal of Environmental and Engineering Geophysics*, *21*(2), 79–87. https://doi.org/10.2113/JEEG21.2.79

Wynn, P. M., Morrell, D. J., Tuffen, H., Barker, P., Tweed, F. S., & Burns, R. (2015). Seasonal release of anoxic geothermal meltwater from the Katla volcanic system at Sólheimajökull, Iceland. *Chemical Geology*, *396*, 228–238. https://doi.org/10.1016/j.chemgeo.2014.12.026

Yurkov, V. V, & Beatty, J. T. (1998). Aerobic Anoxygenic Phototrophic Bacteria. *Microbiology and Molecular Biology Reviews*, *62*(3), 695–724. https://doi.org/10.1128/MMBR.62.3.695-724.1998

Zhang, L., Algeo, T. J., Cao, L., Zhao, L., Chen, Z. Q., & Li, Z. (2016). Diagenetic uptake of rare earth elements by conodont apatite. *Palaeogeography, Palaeoclimatology, Palaeoecology*, *458*, 176–197. https://doi.org/10.1016/j.palaeo.2015.10.049

Blakney, G. T., Hendrickson, C. L., & Marshall, A. G. (2011). Predator data station: A fast data acquisition system for advanced FT-ICR MS experiments. *International Journal of Mass Spectrometry*, *306*(2–3), 246–252. https://doi.org/10.1016/J.IJMS.2011.03.009

Krause-Jensen, D., Marbà, N., Sanz-Martin, M., Hendriks, I. E., Thyrring, J., Carstensen, J., et al. (2016). Long photoperiods sustain high pH in Arctic kelp forests. *Science Advances*, *2*(12), e1501938. https://doi.org/10.1126/sciadv.1501938